Advanced Sensors Towards Ubiquitous Power Internet of Things

Jinliang He, *Fellow*, *IEEE*, *Fellow*, *CSEE*, Zhifei Han, *Student Member*, *IEEE*, and Jun Hu, *Member*, *IEEE*

***Abstract*—The ubiquitous power Internet of Things (UPIoT) uses modern information technology and advanced communication technologies to realize interconnection and human-computer interaction in all aspects of the power system. UPIoT has the characteristics of comprehensive state perception and efficient information processing, and has broad application prospects for transformation of the energy industry. The fundamental facility of the UPIoT is the sensor-based information network. By using advanced sensors, Wireless Sensor Networks (WSNs), and advanced data processing technologies, Internet of Things can be realized in the power system. In this paper, a framework of WSNs based on advanced sensors towards UPIoT is proposed. In addition, the most advanced sensors for UPIoT purposes are reviewed, along with an explanation of how the sensor data obtained in UPIoT is utilized in various scenarios.**

***Index Terms*—Advanced sensors, ubiquitous power Internet of Things, wireless sensor networks.**

I. Introduction

WITH increasing challenges in the energy development process, energy Internet has become a major innovation and development trend to promote transformation of the world's power and energy systems [1]. The essence of the energy Internet is deep integration of energy flow and information flow. It means a deep perception and control of the energy network situation through information technology.

Smart grid is the basis for energy flow in the energy Internet [2]–[4]. Compared with a traditional power grid, smart grid exhibit significant diversity: 1) diversity of power sources, including distributed microgrids, large-scale new energy storage technologies, intermittent renewable energy such as wind and solar energy, etc; 2) diversity of load, including electric vehicles, wireless charging devices, etc; 3) diversity of power grid patterns, including high-voltage transmission networks, medium-voltage distribution networks and distributed microgrids; 4) diversity of information links, including various types of intelligent sensors, communication equipment and other information systems.

The ubiquitous power Internet of Things (UPIoT) is the basis for information flow in the energy Internet [5]. It is important for two-way interaction of information flow and energy flow. UPIoT is an industrial Internet based on sensing, communication and information technologies. It can realize real-time monitoring and regulation of key nodes and key equipment of all levels of transmission and distribution systems. In the energy Internet, the semaphores that need to be perceived are increasing in magnitude with access of a large number of distributed power sources, loads, etc. Therefore, the sensor network in UPIoT presents significantly different technical characteristics from the information monitoring system in the traditional power grid.

In the advanced sensors based WSNs towards UPIoT, we reviewed the most advanced sensors for UPIoT application, described the infrastructure of WSNs for UPIoT purpose, and explained application of sensor data acquired in UPIoT in this paper.

II. Advanced Sensors for UPIoT

Sensors of different types are being developed for various data collection tasks for UPIoT. Concretely, the sensors, categorized by sensing target, include current sensors, voltage sensors, temperature sensors, humidity and gas sensors and so on. Requirements of these sensors are introduced.

A. Requirements of Sensors

In order to deploy WSNs for applications in UPIoT, the sensors need to withstand harsh environmental conditions and ensure a stable supply of energy. Some advances in design and manufacturing of sensors may facilitate deployment of WSNs in power systems and energy internet.

a) Miniaturization of sensors and related devices: Size of measurement units sometimes limits their usage in specific situations. For instance, sizes of traditional voltage and current transformers are relatively large, such that the number of measurement points is limited. Recent progress in MEMS technologies has enabled development of small-sized current and voltage sensors [6]. In [7], the authors proposed a smart-grid-application oriented contactless current sensor that can be easily installed and removed. The trend of miniaturization of sensors would enable an increased volume of data to be collected.

b) Low power consumption: An obstacle for deploying sensors in remote areas is power supply cannot be guaranteed. Infrastructure of power and energy systems, however, is often

Manuscript received July 13, 2023; revised October 19, 2023; accepted November 22, 2023. Date of online publication December 28, 2023; date of current version December 31, 2023. This work was supported in part by the National Natural Science Foundation of China (No. 51921005).

J. L. He (corresponding author, email: hejl@tsinghua.edu.cn; ORCID: https://orcid.org/0000-0002-4458-5026), Z. F. Han and J. Hu are with the State Key Lab of Power Systems, Department of Electrical Engineering, Tsinghua University, Beijing 100084, China.

DOI: 10.17775/CSEEJPES.2023.05850

located in remote areas. Thus, a WSN as a whole is expected to consume as little power as possible. For instance, adopting higher data rate shortens active periods, thus reducing energy consumption of sensor nodes [8]. An alternative approach for power supply is to obtain energy from fields surrounding power lines [9].

c) Low cost: The ever-lowering cost of sensors means more sensors can be deployed, and more data can be collected. Power grids can be more and more transparent to the operators if more data can be collected. Redundant signals provided by WSNs can enable data analysis in a hierarchical manner, thus improving reliability of the analysis.

Sensors of different types are being developed for various data collection tasks in UPIoT. Concretely, quantities that can be measured by sensors include current (magnetic field), voltage (electric field), temperature, humidity, pressure, deformation, and motion etc. Certain gasses can also be detected by corresponding sensors. The following are brief information about different types of sensors that may be applied in UPIoT:

a) Current (Magnetic Field) sensors: The most widely used current measurement devices are current transformers. Rogowski coil current sensors and Hall effect current sensors are also commonly used. In addition, fiber-optic current sensors and giant magnetoresistance (GMR)-based current sensors are being employed for smart grid applications.

b) Voltage (Electric Field) sensors: Traditionally, voltage transformers are the main devices for voltage measurement in power systems. Recently, contactless electric field measurement-based voltage sensors are gaining attention, for they are smaller in size, less costly, and can easily be deployed in a distributed manner. Optical electric field sensors, piezoelectrical electric field sensors and micro electromechanical system (MEMS) electric field sensors are examples of contactless voltage sensors.

c) Temperature sensors: In addition to infrared detectors and thermistor temperature sensors, other types of temperature sensors include distributed fiber-optic temperature sensors, fiber Bragg grating (FBG) temperature sensors, and surface acoustic wave (SAW) temperature sensors. In particular, distributed fiber-optic sensors can be used in a variety of power system applications (e.g., temperature sensing of cables, transformers, and rotating machines), and continuous temperature distribution profiles can be provided [10]. The distributed nature of these sensors means they can be well adapted to WSN architectures.

d) Humidity and Gas sensors: Silicon carbide-based gas sensors, nanomaterial (e.g., carbon nanotube)-based humidity and gas sensors, SAW humidity and gas sensors, and electronic noses are some types of the commonly used humidity and gas sensors. For instance, dissolved gasses in power transformers can be detected non-invasively by nanomaterial gas sensors [11].

e) Deformation sensors: Thanks to development of advanced materials, giant magnetoimpedance-based, nanomaterial-based, fiber-optic material-based, piezoelectric semiconductor-based, magnetostrictive material-based, polymeric piezoelectric material-based, polyimide-based, amorphous alloy-based, and SAW pressure and deformation sensors have been developed. For example, an FBG-based sensor system for wind turbine operational load monitoring is described in [12].

f) Motion sensors: Motion sensors can be used to detect the vibration, acceleration, rotation or displacement of an object. Vibration sensors can be based on deformation sensors, while rotation sensors can be based on magnetic field sensors. Recently, an acceleration transducer with double axis or triaxis and gyroscope have been widely used in sports bracelets and smart phones to capture human body's action, which can also be deployed to detect motion of electric equipment such as wire dancing.

B. Current and Magnetic Field Sensors

According to the principle of sensors, current sensors can be divided into four categories: 1) Connect a small sampling resistor in series in the circuit, measure voltage across the resistor and current can be calculated according to Ohm's law; 2) Through electromagnetic induction coupling, current is calculated by measuring current on the secondary side according to the law of electromagnetic induction; 3) According to the Ampere loop law, using a magnetic field sensor to measure the magnetic field generated by current, then calculating the current; 4) According to Joule's law, measuring the thermal effect of current through a temperature sensor, then calculating the current [13]–[15].

1) Current Sensors Based on Sampling Resistor

This type of measuring equipment uses shunt or coaxial current shunt to measure current. Current is measured by measuring voltage across the sampling resistor which is connected in series in the circuit. In order to improve measurement accuracy, high-precision, low-temperature coefficient resistors are usually selected. This type of measurement technology can measure both AC and DC currents [16]. However, since the sampling resistor is connected to the circuit, it will affect the circuit and thermal effect will increase error [17]. In addition, it cannot be applied to high frequency measurement due to the skin effect and parasitic parameters of the sampling resistor [18]. The sampling resistor method is mainly used in fields of direct current, precision current and inrush current measurement.

2) Current Sensors Based on the Law of Electromagnetic Induction

The Rogowski coil consists of an air-core coil and an integrator. A typical structure of Rogowski was shown in Fig. 1. Measured current passes through the air-core coil. When current changes, electromotive force is induced at both ends of the coil. Voltage signal output through the integrating circuit is linear with measured current. Rogowski coil is simple in structure, low in cost, low in temperature drift and reliable in performance. It can even be integrated on printed circuit boards [19], [20]. Because there is no iron core, there is no saturation and frequency response is fast [21], [22]. However, DC current cannot be measured, and bandwidth is limited. The Rogowski coil is mainly used in high frequency and high current applications.

3) Magnetic Field Sensors

Current can be calculated by using a magnetic field sensor to measure the magnetic field generated by current. The main

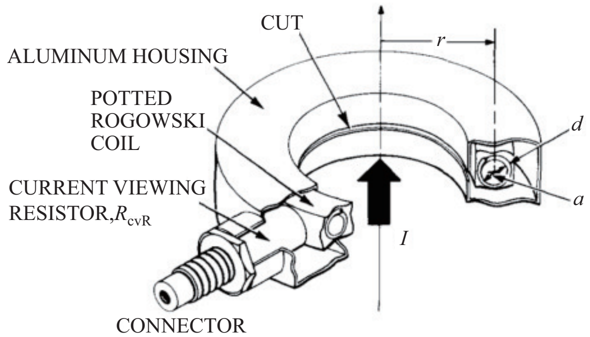

Fig. 1. Typical Rogowski coil. I is the current threading the coil, r is the mean major radius, a is the mean minor radius, and d is the wire diameter. © [1980] AIP Publishing. Reprinted, with permission, from [22].

principles of sensors include electromagnetic induction, fluxgate, Hall effect, magnetoresistance effect, magneto-optical effect, nuclear magnetic resonance and superconducting effect [23], [24]. Sensors with different principles have specific advantages and disadvantages and are suitable for specific occasions.

a) The Search Coil Magnetometer: The Search Coil Magnetometer (SCM) includes a coil, a shield case, and a magnetic core. According to Faraday's law of electromagnetic induction, when magnetic flux passing through the coil changes, an electromotive force is induced at both ends of the coil. Sensitivity of the search coil depends on coil area, number of turns and magnetic permeability of the core. For practical use, the search coil is usually connected to an active signal modulation circuit. Detection coil can only measure AC magnetic field. In special occasions, the coil can be periodically vibrated or rotated for DC magnetic field applications. Detection coil is simple in structure and reliable in performance. It is widely used in space science and high frequency applications [25], [26]. A breakout view of a search coil was shown in Fig. 2.

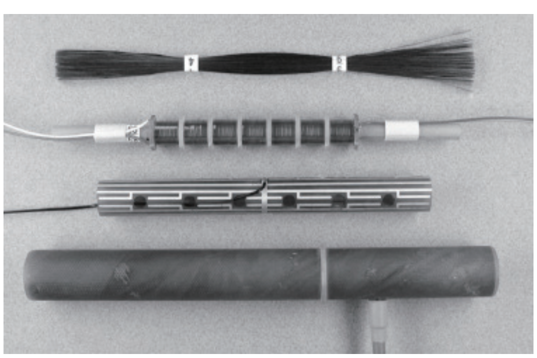

Fig. 2. Breakout view of one search coil. From top to bottom: Stacked strips of permalloy, epoxy mandrel and winding, electrostatic shield, and potted search coil in final epoxy tube. © [2005] AIP Publishing. Reprinted, with permission, from [26].

b) The Fluxgate Magnetometer: Fluxgate magnetometer uses a magnetic core to modulate measured magnetic field under saturation excitation of an alternating magnetic field. Magnetic field strength of the core has a nonlinear relationship with measured magnetic field. The fluxgate magnetometer includes a magnetic core, an excitation coil, and an induction coil. Under saturation excitation of the alternating magnetic field, core magnetic permeability is cyclically transformed at a double frequency. According to Faraday's law of electromagnetic induction, the electromotive force of the induction coil is proportional to flux change rate [27]. According to even harmonic component, pulse amplitude difference and pulse time interval of output signal, measured magnetic field strength can be calculated. Through the differential magnetic circuit structure design, the odd-order component of the output can be eliminated and sensitivity is improved [28]. The fluxgate magnetometer has a simple and reliable structure and can measure the magnetic field vector in three directions of space. It has obvious advantages in low frequency weak magnetic fields. It is widely used in geomagnetic research, navigation systems, space science and high-speed motion systems [29].

c) Magnetic Field Sensor Based on Hall Effect: When charged particles move inside a magnetic field, the Lorentz force is exerted to the particles, which deflects charged particles and causes them to accumulate at the surface of the conductor, resulting in an electromotive potential perpendicular to direction of the particles' movement. When the electromotive force generated by electromotive potential is balanced with the Lorentz force, electrons will pass through the conductor without deflection. This electromotive potential is referred to as Hall potential. The Hall effect in semiconductors is significant. Sileo L. *et al.* proposed three-axis magnetic sensors which are fabricated through large-scale integration processes and semiconductor processes [30]. A schematic of the three-axis Hall sensor was shown in Fig. 3. By optimizing the magnetic circuit design and integrating a micro flux concentrator, sensitivity of Hall devices can be increased [31]. In general, measurement range and the frequency range of Hall devices are $10^{-7} \sim 10$ T, and DC $\sim 10^5$ Hz, respectively.

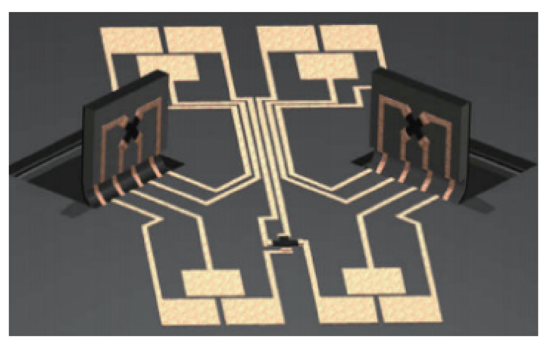

Fig. 3. The schematic of the three-axis Hall sensor. © [2010] Elsevier. Reprinted, with permission, from [30].

d) Magnetoresistive Sensor: Magnetoresistive materials include iron, cobalt, nickel, and other ferromagnetic metals, metal alloys and semiconductors. Resistances of materials change when a magnetic field is applied. The magnetoresistance effect includes the anisotropic magnetoresistance (AMR) effect, giant magnetoresistance (GMR) effect, giant magnetoimpedance (GMI) effect, tunneling magnetoresistance (TMR) effect and colossal magnetoresistance (CMR) effect [32], [33].

i) AMR effect. The anisotropic magnetoresistance in ferromagnetic materials has a magnetoresistance effect related to the included angle between current and magnetic field directions. The anisotropic magnetoresistance effect is caused by spin-orbit coupling and low-symmetry potential scattering centers in magnetic materials and is closely related to anisotropic scattering of localized d-electrons and s-electrons [34].

ii) GMR effect. The GMR effect was first discovered in [Fe/Cr]n periodic antiferromagnetic coupling multilayer films in 1988. Due to its large magnetoresistance ratio compared with that of anisotropic magnetoresistors, this effect is called the giant magnetoresistance effect. Its composition mainly includes the reference layer and the magnetic free layer (e.g., Co, CoFe, CoFeSi, and CoFeMnSi) and the non-magnetic metal layer (e.g., Cu, Cr, Ag, and Ru) sandwiched in between. Resistivity change of the Fe/Cr multilayers can reach 42% at room temperature [35]. High-performance GMR sensors can also be obtained in combination with highly magnetostrictive $Fe_{50}Co_{50}$ [36]. In terms of the relationship between current and the sensor's surface, the structure can be divided into "current parallel to membrane surface" (CIP) and "current perpendicular to membrane surface" (CPP) structures. Compared with CIP-GMR structure, the CPP-GMR structure has advantages of small volume, low junction resistance and high signal-to-noise ratio [37]. For distributed measurement of power grid, GMR current sensor has broad application prospects. Compared with traditional electromagnetic current transformers, it can measure DC to high frequency (MHz order) current signal. Compared with Hall element, it has advantages of small volume, high sensitivity and better temperature stability, which can adapt to drastic changes of environmental temperature. In addition, it has advantages of simple structure and low cost, which facilitates large-scale promotion.

iii) GMI effect. The GMI effect refers to the phenomenon that AC impedance of a material changes significantly with applied magnetic field. The GMI effect was discovered by Panina and Mohri in Co-based amorphous wires in 1994. Because of its advantages of high sensitivity, fast response and high stability, the GMI effect has large application potential in applications such as sensor technology and magnetic recording technology, especially development of high sensitivity miniaturized magnetic sensors. The GMI effects have also been discovered in amorphous films, glass-coated amorphous metallic wires, and amorphous metallic ribbons.

iv) TMR effect. When an ultra-thin insulating barrier layer is used instead of a non-magnetic metal layer, conductive electrons may go through the insulating barrier via quantum tunneling, wherein the probability of tunneling depends on the relative orientation of magnetic moments of the two magnetic layers.

v) CMR effect. The perovskite-structured manganese oxide has a spin polarizability near 100%, exhibits a huge magnetoresistance effect near the ferromagnetic Curie temperature, which is called the CMR effect. Research on CMR still face some problems: The magnetoresistive effect of manganese oxide is only significant at high magnetic fields or low temperatures. Compatibility problems with silicon technology also limit application of manganese oxide devices. After solving these problems, the CMR effect will be of great significance in basic research and related electronic device applications.

e) Magneto-optical Effect Magnetic Sensor: Magneto-optical effect magnetic sensors are mainly divided into two categories:

Magneto-optical Magnetometer based on the Faraday effect or the Kerr effect. When a beam of polarized light passes through the Faraday crystal, the plane of polarization rotates under action of a magnetic field. Magnitude of the magnetic field can be calculated by measuring polarization angle of the light [38], [39].

Fiber-optic Magnetometer is based on the magnetostrictive effect of the fiber. Fiber interference sensor uses one beam of light to pass through two equal length fibers. One fiber is the reference fiber, and the other fiber is the induction fiber. Under the magnetic field, magnetostriction of the induction fiber is slightly deformed while reference fiber is not affected by the magnetic field. Microscopic deformation of the fiber can be measured by interference to calculate the magnetic field [40], [41]. Basic elements of a single-axis fiber-optic magnetometer utilizing a magnetostrictive sample was shown in Fig. 4.

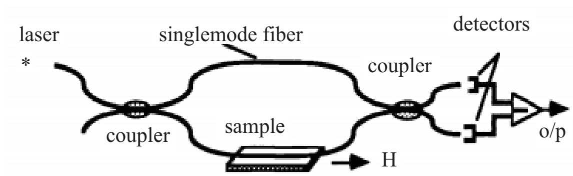

Fig. 4. Basic elements of a single-axis fiber-optic magnetometer utilizing a magnetostrictive sample. © [1995] SPIE. Reprinted, with permission, from [41].

Structure of magneto-optical effect magnetic sensors is simple and reliable. Sensors are small in size, light in weight, and have good linearity and large dynamic range. However, optical devices are difficult to manufacture. In addition, it faces the problem of long-term stability and temperature stability.

f) Nuclear Precession Magnetometer: The Nuclear Precession Magnetometer is based on the principle of magnetic resonance. Spins of electrons and nuclei with an odd number of nucleons in an atom have angular momentum and magnetic moment. Ratio of the magnetic moment to angular momentum is magnetic rotation ratio γ, which is constant for a particular atom. Under an external magnetic field, the nuclei or electrons precess. When an RF magnetic field is added in the vertical direction and satisfies the corresponding conditions, the atom will produce magnetic resonance [42]. For a specific sample, under an external magnetic field, frequency of the RF field is adjusted to cause magnetic resonance. The external magnetic field can be accurately measured by measuring frequency of the RF field at resonance [43]. This method is mainly suitable for magnetic fields of medium field strength and extremely low frequency.

g) Super-conduct Quantum Interfere Device: Super-conduct Quantum Interfere Device (SQUID) is based on flux quantization and Josephson tunnelling. Extremely small flux changes can also cause voltage changes across the Josephson junction. This kind of device is currently the most sensitive magnetic flux sensing devices, and is widely used in biomedical, superconducting materials, geological exploration and other fields. With development of high-temperature superconductors and Josephson junction manufacturing process, such sensors will have broad application prospects [44], [45].

Magnetic field strength and frequency range measured by various types of magnetic sensors are shown in Table I.

TABLE I
MAGNETIC FIELD STRENGTH AND FREQUENCY RANGE MEASURED BY VARIOUS TYPES OF MAGNETIC SENSORS

Type of sensors	Field strength (T)	Frequency (Hz)
Search Coil Magnetometer	10^{-14}–10^{3}	10^{-1}–10^{9}
Fluxgate Magnetometer	10^{-13}–10^{-3}	0–10^{4}
Magnetic Field Sensor Based on Hall Effect	10^{-7}–10	0–10^{5}
Magneto-optic Magnetometer	10^{-4}–10	0–10^{9}
Fiber-optic Magnetometer	10^{-9}–10^{-3}	0–10^{5}
Nuclear Precession Magnetometer	10^{-4}–10^{-1}	0–10^{0}
Super-conduct Quantum Interfere Device	10^{-15}–10^{-7}	0–10^{6}
AMR Sensor	10^{-6}–10^{0}	0–10^{5}
Multilayer GMR Sensor	10^{-9}–10^{0}	0–10^{9}
Spin Valve GMR Sensor	10^{-11}–10^{-3}	0–10^{9}
TMR Sensor	10^{-12}–10^{-1}	0–10^{9}

A variety of non-contact current sensors can be developed based on magnetic sensors [46]–[50]. For open-loop current sensors, current is calculated by measuring the magnetic field generated by current based on the Ampere loop law. For closed-loop current sensors, zero-flux technology is basically used, so the magnetic field sensor works near the zero point, thus can reduce hysteresis, temperature drift, and increase frequency response. Current passes through the core, and magnetic sensor output in the air gap of the core acts as an error signal. The coil wound on the core is driven by the power amplifier, and the magnetic field generated by the current in the coil compensates for the magnetic field generated by current being measured. When the magnetic field is fully compensated, current in the coil is proportional to current to be measured. The coil current can be measured by the sampling resistor, thereby calculating measured current. In low frequency cases, frequency response depends on electronic components in the sensor. At high frequencies, frequency response can be compensated due to the transformer effect of the coil [51]. The main disadvantages of this type of closed-loop current sensors are complex structure, high cost, large volume and high energy consumption.

Comprehensive performance of various current sensors is shown in Table II. The widely used current transformer can only measure power frequency current and cannot realize distributed monitoring. Hall sensor, fiber optic current sensor and magneto-optical current sensor can realize wide-band current measurement. Hall sensor is simple in structure and low in price. It is widely used in occasions where accuracy is not very high. The disadvantage of the Hall sensor is it is susceptible to external magnetic field and current direction. Fiber optic current sensors are expensive and cannot be used for distributed monitoring. Magneto-optical current sensor has the disadvantages of bulk and it is more expensive than fiber optic current sensor. Fluxgate current sensors are mainly used for extremely high frequency currents and very small current measurements, but they are only used in high precision fields such as medical fields and standard measurement due to their high price and large size. The giant magnetoresistive sensor has the advantages of high integration, high sensitivity, small size, low cost, small temperature drift and wide measurement range. In the ubiquitous power IoT, distributed current monitoring sensors can be selected according to specific applications.

C. Voltage and Electric Field Sensors

Traditional voltage measuring equipment of a power system is voltage transformer. Voltage to be measured is calculated by using current value of reference resistor. Voltage transformers based on this principle can only provide power frequency voltage information. Transient voltage and DC voltage cannot be measured accurately. Moreover, these devices are bulky and cannot meet distributed installation and real-time monitoring required by ubiquitous power IoT.

According to the Gaussian algorithm, voltage value can be depressed with electric field of three fixed sensing nodes in space. Therefore, voltage measurement based on non-contact electric field sensors has drawn great attention.

Electric field sensors are voltage measuring devices that do not invade the primary system. Integrated electric field sensors integrate back-end processing circuits such as electric field bias and temperature compensation into the sensor which can reduce device size and facilitate wide use of the sensors. Integrated electric field sensors mainly use principles of electro-optic effect, inverse piezoelectric effect, electrostatic induction, etc. Integrated electric field sensors are suitable for voltage measurement in ubiquitous power IoT for they are smaller in size, low in cost, and can be deployed in a distributed manner. This section mainly introduces electric field sensors which can be used in voltage measurement. Parameters of electric field sensors based on various principles are shown in Table III.

TABLE II
COMPREHENSIVE PERFORMANCE OF VARIOUS CURRENT SENSORS

Type of sensors	Current (A)	Frequency (Hz)	Nonlinearity (%)	Temperature drift coefficient (ppm/K)
Sampling Resistor Current Sensor	10^{-2}–10^{4}	0–10^{7}	0.1–2	25–300
Rogowski Coil	10–10^{5}	10^{4}–10^{9}	0.2–5	50–300
Magneto-optical Current Sensor	1–10^{4}	0–10^{9}	0.1–1	1000–4000
Fluxgate Magnetometer	10^{-3}–10^{3}	0–10^{4}	0.001–0.5	<50
Hall Effect Current Sensor	1–10^{4}	0–10^{5}	0.5–5	200–2000
GMR/TMR Current Sensor	10^{-4}–10^{5}	0–10^{9}	0.01–0.5	100–1000

TABLE III
PARAMETERS OF ELECTRIC FIELD SENSORS BASED ON VARIOUS PRINCIPLES

Type of sensors	Field strength	Frequency (Hz)	Resolution (V/m)
Electric Field Sensor Based on Electro-optic Effect for Low Electric Field [59]	$E_{min} = 22$ mV/m	10^{10}	0.02
Electric Field Sensor Based on Electro-optic Effect for High Electric Field [64], [65]	$E_{max} = 1$ MV/m	10^8	500
Electric Field Sensor Based on Inverse Piezoelectric Effect [72]	$E_{max} = 1570$ kV/m	10^5	12.7
Electric Field Sensor Based on MEMS [84]	$E_{max} = 230$ kV/m	300	100
Electric Field Sensors Based on Electrostatic Force [86]	$E_{max} = 700$ kV/m	10^3	172

1) Electric Field Sensors Based on Electro-optic Effect

Electric field sensors based on electro-optic effect are currently widely studied. Using electro-optical crystals, an electrical signal can be converted into an optical signal, and then the electric field to be measured can be measured by optical methods. Applied electric field causes a change in the refractive index of the electro-optic crystal or causes birefringence. Commonly used photoelectric crystals include BGO, $LiNbO_3$, ADP, etc. According to the relationship between refractive index and electric field, the electro-optical effect can be divided into Pockels effect and Kerr effect. Pockels effect is widely used due to its good linearity. This type of integrated optical electric field sensor has high response speed, wide frequency bandwidth and high resolution.

Bulmer *et al*. studied and reported the optical electric field sensor for the first time at the NRL [52]–[56]. The reported electric field sensor was based on the Mach-Zehnder Interferometer and typical structure was shown in Fig. 5. When linearly polarized light passed through the channel, it was first divided equally into two by the first Y-branch. One beam of light entered the optoelectronic crystal such as $LiNbO_3$ and was located in the electric field to be measured, and the other beam was used as a reference. According to the Pockels effect, the refractive index of the waveguide channels 1 and 2 were different, resulting in a phase different between the two polarized lights. The two polarized lights were finally superimposed by the second Y-branch, and the obtained polarized light amplitude was related to the phase difference between the two beams, that is, an amplitude-modulated optical signal is output. Resolution of the sensors reached 1 V/m and bandwidth reached 300 MHz.

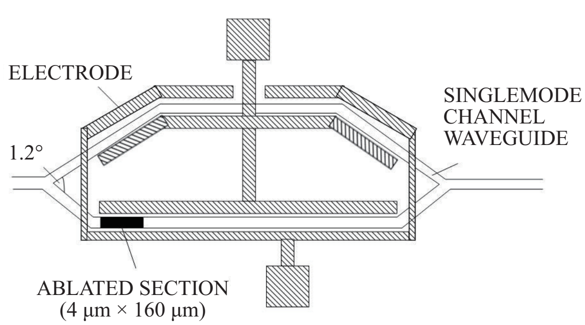

Fig. 5. Typical structure of electric field sensor based on the Mach-Zehnder Interferometer. © [1995] IEEE. Reprinted, with permission, from [56].

At first, this type of sensor was only suitable for low electric fields. Tajima *et al*. at NTT Corp. reported optical electric field sensors with a resistive antenna to improve bandwidth [57]–[59]. Sensors could reach a minimum detectable field of 22 mV/m and a bandwidth of over 10 GHz. At the same period, Petermann *et al*. at Berlin University of Technology located the antenna along the waveguide [60]–[63] and got a resolution of 1 mV/m and a bandwidth of 3 GHz.

In order to measure electric fields of high amplitude and wide bandwidth, Zeng *et al*. at Tsinghua University optimized structure of the electrode and antenna [64]. Using different electrodes and antennas, reported sensors had half-wave electric field ranges from 10 kV/m to 100 kV/m. Bandwidth of measurement could reach 100 MHz. They also developed optical electric field sensors with mono-shielding electrodes [65]. Sensors had half-wave electric field ranges from 2000 kV/m to 8000 kV/m.

In addition to electric field sensors based on the Mach-Zehnder Interferometer, there are also some other optical electric field sensors. In 1988, an optical electric field sensor based on Coupler Interferometer was proposed by Howerton *et al*. [66]. Zeng *et al*. reported a new kind of optional electric field sensor based on Coupler Interferometer [67]. It could be used in intense electric field measurement (up to 1000 kV/m) and has a better optical bias control.

Electric field sensors based on Common Path Interferometer (CPI) was first proposed by Jaeger *et al*. [68]. Takahashi *et al*. proposed electric field sensors with a half-wave electric field of 100 MV/m [69], [70]. Zeng R. *et al*. improved sensitivity and half-wave electric field by locating antennas and electrodes around the waveguide [71].

2) Electric Field Sensors Based on Inverse Piezoelectric Effect

Polarization and lattice displacement of piezoelectric materials in electric fields causes mechanical deformation of material, which converts electrical energy into mechanical energy. The electric field can be measured by measuring displacement of the material. There are several ways to measure deformation of the piezoelectric material.

He *et al*. at Tsinghua University proposed an electric field sensor with broad bandwidth and large dynamic range [72]. Deformation of the piezoelectric material was measured with piezoresistive effect. Structure of the sensor was shown in Fig. 6. In the electric field, the piezoelectric crystal deformed, and deformation would be transmitted mechanically to the coupled semiconductor membrane. Piezoresistive materials of specific shapes were prepared by doping on the semiconductor membrane. The piezoresistive effect converted stress in the membrane into a change in resistivity of the piezoresistive materials. A Wheatstone Bridge was used to measure resistivity

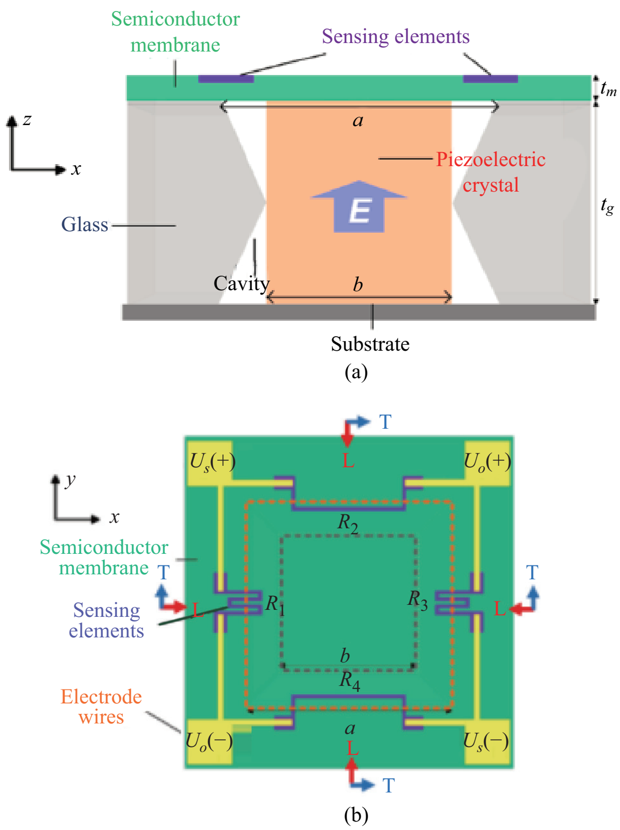

Fig. 6. Structure of electric field sensor based on inverse piezoelectric effect and piezoresistive effect. © 2020 IEEE. Reprinted, with permission, from [72]. (a) Cross-section view, (b) Overhead view.

changes of piezoresistive materials. Bandwidth of the sensor was DC–100 kHz and magnitude of measurement reached 15.7 kV/cm. Resolution under DC-field was about 12.7 V/m.

He *et al.* also measured deformation of the piezoelectric material through a way of capacitance measuring [73], [74]. Two piezoelectric polymer layers with opposite polarization directions were stacked together and fixed at both ends. The layers formed the upper electrode of the capacitor. The lower electrode of the capacitor was fixed. In the electric field, the piezoelectric layer was bent, causing capacitance to change. The electric field could be measured by measuring change in capacitance.

Using optical methods to detect deformation of piezoelectric materials is another way used in electric field sensors. Deformation of optical device changes parameters such as wavelength. By coupling the piezoelectric material to an optical device such as a grating, mechanical deformation of the piezoelectric material can be converted into an optical signal [75]–[78].

3) Electric Field Sensors Based on Micro Electro-Mechanical System

Micro Electro-Mechanical System (MEMS) is a system integrated by mechanical elements, sensors, actuators and electronic devices. The MEMS devices are generally fabricated on a common substrate through microfabrication technology.

In 2003, Riehl *et al.* at UC Berkeley proposed a classic MEMS-based electric field sensor [79]. The structure was

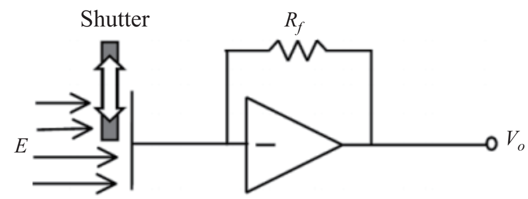

Fig. 7. Structure of electric field sensor based on micromechanical resonators. © [2003] IEEE. Reprinted, with permission, from [79].

shown in Fig. 7. The basic principle of the sensor was mechanical vibration and electric field induction. A grounded shutter periodically moved under control of an excitation source. A measuring circuit is connected to the fixed electrode. When the electric field impinged on the sensor, an induced current was generated on the fixed electrode due to electrostatic induction. Electric field strength could be calculated by measuring magnitude of the induced current. The sensor had a resolution of 630 V/m.

Peng *et al.* at IECAS improved this type of sensor in several ways [80], [81]. They changed the measuring circuit and driving mode, shape, quantity and location of electrodes. The shutter could be driven by piezoelectric effect or be thermally driven. Electrodes could be made into comb shape to improve the response.

Yu *et al.* at Tsinghua University reported MEMS-based electric field sensors that were suitable for HVDC electric fields [82]–[84]. The sensors eliminated measurement errors caused by ion flows at the vicinity of HVDC lines.

Kainz *et al.* proposed a distortion-free sensor based on MEMS [85]. Structure of the sensor is shown in Fig. 8. Under electric fields, the effect of electrostatic induction generated internal forces of the MEMS devices. Internal forces caused displacement of a spring-suspended mass. By optically measuring displacement of the mass, the electric field could be measured. Resolution of the sensor was about 100 $\text{Vm}^{-1}\text{Hz}^{-1/2}$ with a quasi-static regime $\leq$ 300 Hz and a measurement range of tens of kV/m.

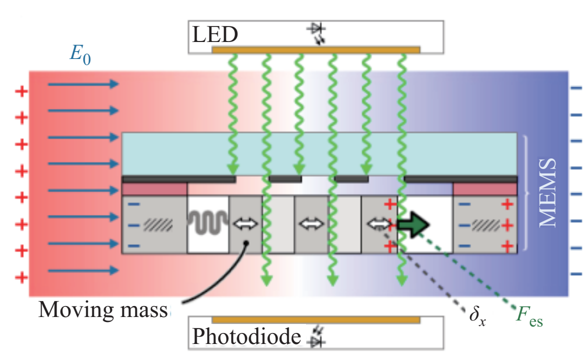

Fig. 8. Structure of distortion-free MEMS electric field sensor. © [2018] Springer Nature. Reprinted, with permission, from [85].

4) Electric Field Sensors Based on Electrostatic Force

In an electric field, sensor structure is subjected to an electrostatic force due to induced charges. Electric field measurement can be achieved by using electrostatic force to actuate sensor components. Structure of an electric field sensor

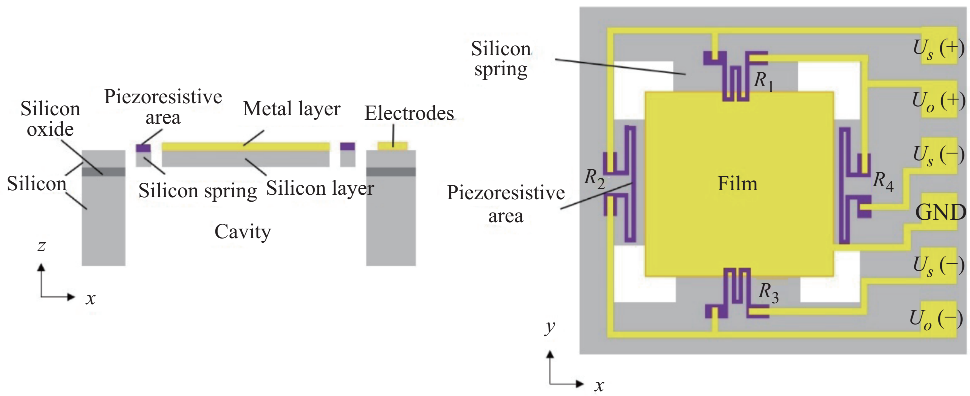

Fig. 9. Structure of electric field sensor with electrostatic field bias. © [2022] IEEE. Reprinted, with permission, from [86].

using piezoresistive effect coupled with electrostatic force was shown in Fig. 9 [86].

Sensor film consists of a silicon layer and a grounded metal layer. The membrane was connected to the surrounding fixed area by silicon springs. A piezoresistive doped region prepared by ion doping was arranged on the silicon spring. The piezoresistive doped regions were connected by metal electrodes to form a Wheatstone bridge structure. Under action of the electric field, the metal layer vibrated under action of electrostatic force, driving the silicon spring to vibrate to generate stress. Under stress, resistance of the piezoresistive doped region changed, which was converted into a differential signal by the Wheatstone bridge. The device exhibited an ac resolution of 172 V/m/Hz$^{1/2}$ and a linear measurable electric field range of 312 V/m to over 700 kV/m. Structure of the electric field sensor can also be designed as a cantilever structure [87].

Huang *et al*. at Tsinghua University proposed a new kind of electric field sensor based on electrostatic force [88]. The structure was shown in Fig. 10. The sensor consisted of a silicon cantilever bonded with a mass and a PTFE electret layer. The electret layer could provide electrostatic field bias when charged. A piezoelectric film was coated on the cantilever. In electric fields, the cantilever would bend due to electrostatic attraction, which would cause the piezoelectric film to deform. Deformation could be read out through the piezoelectric effect

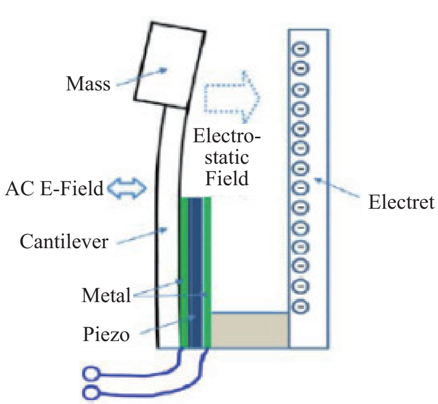

Fig. 10. Structure of electric field sensor with electrostatic field bias. © [2017] IEEE. Reprinted, with permission, from [88].

of the piezoelectric film. The sensor had a sensitivity of 15.8 mV/(kV/m) and a resolution of about 20 V/m. The sensor had the advantage of low power consumption.

Chen *et al*. at University of Manitoba reported another electric field sensor based on electrostatic force [89]. A membrane mirror suspended by micro springs was fabricated. In electric fields, the membrane would be displaced vertically under the influence of electrostatic force. By measuring displacement of the membrane with a laser position sensor, electric field strength can be measured. The reported sensor could reach a sensitivity of 360 mV/(kV/m) and a resolution of 17 V/m. At the resonance point, the resolution could reach 0.1 V/m.

Voltage sensors based on electroluminescent materials measures voltage by measuring the change in light intensity of materials under the influence of voltage [90], [91]. Such sensors still need further study in terms of light intensity measurement and sensor stability. In addition, voltage and electric field sensors based on biofilm or thermoelectric effects of pyroelectric materials are also possible solutions.

D. Temperature Sensors

In addition to current/magnetic field sensors and voltage/electric field sensors, there are many other kinds of sensors that would be applied to monitoring of ubiquitous power IoT.

Advanced temperature sensors use materials such as high-Curie-point lead-free positive temperature coefficient resistor (PTCR) materials, ferroelectric ceramics materials, shape memory alloy and shape memory polymer materials. Commonly used temperature sensors also include infrared sensors, distributed fiber optic (DFO) sensors, fiber grating sensors, and surface acoustic wave (SAW) sensors. Traditional thermally sensitive resistors can be used to measure a wide range of temperature (up to 2000°C), while SAW and fiber -based temperature sensors have limitations in measuring very high temperatures. However, measurement ranges for these sensors are still suitable for IoT applications. Infrared temperature sensing devices are able to measure temperature within a certain point or area. Distributed optical fiber sensors can monitor distribution of temperature over a long distance along the fiber.

1) High-Curie-point Lead-free PTCR Materials

Thermally sensitive resistors can be categorized into positive temperature coefficient (PTCR), negative temperature coefficient resistor (NTCR), and critical temperature resistor (CTR). Resistance of a PTCR increases dramatically after its temperature exceeds the Curie point. Traditionally, PTCR materials with high-Curie points are realized by adding lead, which is harmful for the environment. Thus, there is an urgent need to find environmentally friendly high-Curie-point Lead-free PTCR materials that can be used as substitutes to Lead-containing materials.

Adding $(Bi_{0.5}Na_{0.5})TiO_3$ (BNT) or $(Bi_{0.5}K_{0.5})TiO_3$ (BKT) to $BaTiO_3$ can increase the Curie point by tens of degrees, by which environmentally friendly thermally sensitive resistor (TSR) temperature sensors with improved performance can be fabricated. Takeda *et al*. rose the Curie point from 130°C to 220°C by adding 50 mol% BNT to $BaTiO_3$ [92]. By doping 5 and 10 mol% BKT, PTCR materials with Curie points of 155°C and 165°C could be obtained [93]. In [94], a PTC material with a Curie point of 155°C and a jump of resistivity (maximum resistivity divided by minimum resistivity) of 4.0 orders of magnitude was achieved by adding BKT. Li *et al*. fabricated a PTCR material whose Curie point and jump of resistivity were 183°C and 4.0 orders of magnitude, respectively, by doping BNT [95].

2) Distributed Fiber-optic (DFO) Temperature Sensor

DFO temperature sensors are based on Rayleigh scattering, Raman scattering, Brillouin scattering and frequency shift effects. With advantages of good insulation properties, low electromagnetic interference, high voltage resistance and high chemical resistance, DFO temperature sensors can simultaneously measure temperature and stress along the optical fiber. The sensors can be used in power plant temperature monitoring, cable tunnel fire monitoring, high-voltage power cable safety monitoring, and other power system applications.

DFO temperature sensor was first proposed by proposed by British researchers in 1980s [96], [97]. Since then, several variants have been developed, such as liquid-core optical fiber distributed temperature monitoring system based on Rayleigh backscattering [98] and fiber temperature measurement system based on either Brillouin Optical Time Domain Analysis (BOTDA) or Brillouin Optical Time Domain Reflectometer (BOTDR) [99].

Soto *et al*. focused on extending sensing distance while maintaining accuracy and developed a 240-kilometer fiber based on BOTDA, half of which used for sensing and the other half for data transmission. The principle of BOTDA is shown in Fig. 11. The fiber had a spatial resolution of 5 m, a temperature resolution of 1.9°C, and a stress resolution of 38 [100]. Dong *et al*. introduced a 150-kilometer optical fiber based on BOTDA with a spatial resolution of 2 m, a temperature resolution of 1.5°C and a stress resolution of 30 in [101]. By optimizing differential pulse-width pair BOTDA, a spatial resolution of 2 cm could be achieved with a temperature resolution of 2°C over a 2 km sensing fiber [102].

3) Fiber Grating Temperature Sensor

Wavelength-encoding characteristic of fiber grating sensors is facilitated by phase grating in the fiber core created based on photosensitivity of optical fiber materials. The most widely used type of fiber grating temperature sensors is fiber Bragg grating (FBG) sensor. The center reflection wavelength of FBG is affected by strain and temperature.

Through Brillouin frequency shift and birefringence of polarization-maintaining optical fiber, Zou *et al*. created a fiber grating sensor with a stress resolution of 3 and a temperature resolution of 0.08°C based on dynamic grating [103]. A birefringence photonic crystal fiber sensor with a temperature sensitivity of 6.6 nm/°C based on fiber loop mirror was introduced in [104]. The temperature sensor proposed by Ahmed *et al*. had a sensitivity of 479.48 pm/°C [105]. Pulido-Navarro *et al*. proposed a type of sensor based on long period fiber gratings that could measure a temperature of 400°C and had a sensitivity of 21 pm/°C [106].

E. Deformation Sensors

There are many types of deformation sensors, such as strain sensors, pressure sensors, displacement sensors, etc. Advanced materials for deformation sensors include nanomaterials, piezoelectric semiconductor materials, magnetostrictive materials, organic polymer piezoelectric materials, ferroelectric electret materials, etc. Fiber based strain sensors, amorphous alloy strain sensors, and SAW pressure sensors are examples of commonly used deformation sensors. Carbon nanotube strain sensor usually has high strain amplitude, while optical fiber strain sensor has the advantages of high-pressure resistance and high acid/alkali resistance. Compared with traditional pressure sensor, polymer pressure sensor is flexible and good in processing performance. Surface acoustic wave pressure sensor has the advantages of passive wireless.

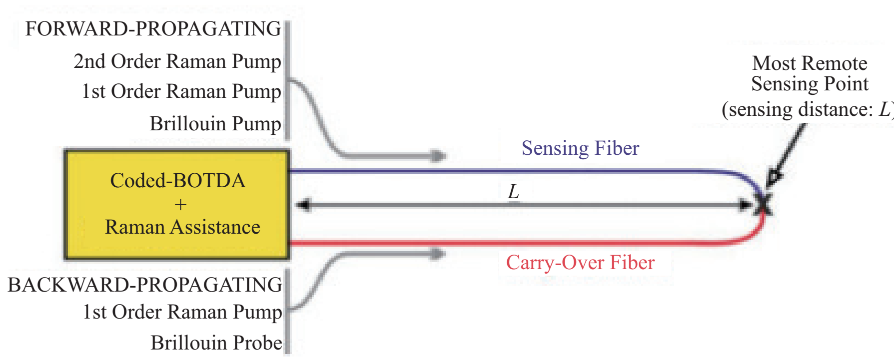

Fig. 11. Schematic diagram showing the principle of a long-range BOTDA sensor employing a linear sensing fiber configuration. © [2014] Optica Publishing. Reprinted, with permission, from [100].

1) Nanomaterial-based Sensor

New nanomaterials such as carbon nanotubes, nanoparticles, nanowires and graphene can be used for strain sensors for applications including building structure monitoring, human health monitoring, bionic robots, etc.

Yamada *et al*. fabricated a resistive strain sensor using single-walled carbon nanotube arrays. The sensor exhibited excellent durability and stability at high strain levels, and was able to measure strains up to 280%, which was 50 times more than conventional metal strain sensors [107]. The structure was shown in Fig. 12. Cai *et al*. fabricated a capacitive transparent strain sensor with single-walled and double-walled carbon nanotube films obtained by floating catalytic chemical vapor deposition (FCCVD). The sensor had good linear response and could detect strains up to 300% [108]. Tadakaluru *et al*. prepared multi-walled carbon nanotube films by chemical vapor deposition (CVD). With natural rubber being the substrate, a sandwich-type resistive strain sensor was fabricated, and it was able to detect strains up to 620% [109].

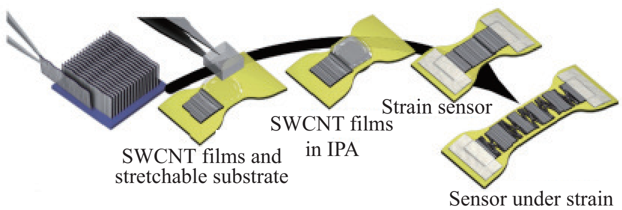

Fig. 12. Structure of the SWCNT strain sensor. © [2011] Springer Nature. Reprinted, with permission, from [107].

2) Fiber-based Sensor

Distributed BOTDA fiber optic strain sensor and FBG strain sensor are hot spots of current research. He *et al*. designed a FBG sensor with a strain resolution of 2.6 nε without strain applied and 17.6 nε with strain applied through the cross-correlation demodulation algorithm [110]. Shen *et al*. proposed a strain sensor based on fiber loop mirror and low-birefringence polarization-maintaining optical fiber, whose strain-temperature coefficient was only 0.094 με/°C [111]. Liang *et al*. invented a type of strain sensor by twisting two optical fibers together [112]. It used microbending losses of the fiber to measure deformation curvature. Xia *et al*. used Mach-Zehnder interferometer for curvature sensing and obtained a sensitivity of -35.41 nm/m^{-1} in the range of 0.6846 m^{-1}–1.0606 m^{-1} [113].

3) Sensors Based on Magnetostrictive Materials

Pasquale reviewed application of CoFeB magnetostrictive material in strain and force sensors [114]. Linearity of magnetostrictive materials could be increased by appropriate magnetic field/stress annealing during preparation or post-processing. Son *et al*. developed a non-contact torque sensor [115]. Negative magnetostrictive ferromagnetic chevrons were bonded on the nonmagnetic object to be measured. Torsional stress resulted in varied magnetizations in the chevrons, which could be measured by the pick-up coils.

4) Sensors Based onPiezoelectric Semiconductor Materials

Piezoelectric semiconductor materials are advantageous in that they are compatible with MEMS fabrication processes and traditional fabrication processes.

Strittmatter *et al*. studied the electromechanical response of Schottky diodes on n-GaN, which was affected by strain frequency and applied DC bias [116]. Results showed the strain measurements above 10 Hz had high sensitivity and the device could be used in small strain detection. Wang studied synthesis of polarized surface-dominated semiconductors and piezoelectric ZnO nanostructures [117]. This structure minimized electrostatic energy due to spontaneous polarization and could be applied to optoelectronics, sensors and resonators.

5) Sensors Based on Acoustic Materials

Sensors based on acoustic materials mainly refer to surface acoustic wave (SAW) sensors. A surface acoustic wave refers to an acoustic wave traveling along the surface of a material. A typical surface acoustic wave sensor includes a piezoelectric substrate and two interdigital transducers at both ends of the substrate. Commonly used piezoelectric substrates include piezoelectric single crystals, piezoelectric ceramics, and piezoelectric films. Piezoelectric single crystals, such as quartz, have the advantages of high reliability and low propagation loss. Piezoelectric ceramics are suitable for low-frequency devices. Piezo films, such as ZnO, are suitable for integration with semiconductor devices. SAW sensors can measure stress, pressure, displacement, acceleration and other quantities. When pressure is applied to the piezoelectric substrate, the stress distribution of the piezoelectric substrate changes. This causes the substrate to deform while the elastic modulus and density of the substrate is also slightly changed. The deformation of the substrate causes the size of the resonator to change, and the variation of the elastic modulus and density of the substrate causes variation of the SAW's velocity. Changes in resonator's size and SAW's velocity eventually cause the center frequency of the resonator to shift, thus change in pressure can be sensed by measuring the offset.

In 2008, Benetti *et al*. proposed a SAW resonator-based pressure sensor [118]. The scheme of the pressure sensor based on SAW resonators was shown in Fig. 13. The sensor's SAW device was a double-ended resonator, and the substrate was ST-cut quartz. Its working frequency was about 393 MHz, the range of pressure test was 0–300 kPa, and resolution was about 3.5 Pa. In 2012, Moulzolft *et al*. proposed a SAW pressure sensor with gallium lanthanum silicate (LGS) crystals as the substrate [119]. It could be applied to high temperature and high-pressure conditions. The sensor passed the test at a high pressure of 225 PSI and a high temperature of 500°C.

F. Gas and Humidity Sensors

Current advanced gas sensors and humidity sensors include silicon carbide-based gas sensors, nanomaterial-based gas sensors and moisture sensors, electronic noses, SAW gas sensors, polyimide film humidity sensors, etc. For gas sensors, traditional metal oxide gas sensors are widely used, but this kind of sensor need to be heated before gas detection. New nanomaterials such as carbon nanotubes, SAW gas sensors and electronic noses can work at room temperature. For humidity sensors, the polymer capacitive humidity sensor is widely used. Polyimide has good stability, temperature resistance,

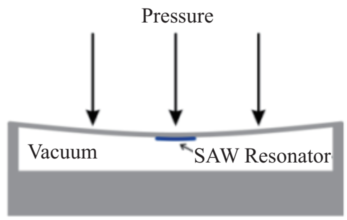

Fig. 13. Scheme of a pressure sensor based on SAW resonators. © [2008] IEEE. Reprinted, with permission, from [118].

corrosion resistance and response speed. New nanomaterials and SAW humidity sensors also have good performance.

1) Sensors Based on Silicon Carbide Materials

The SiC-based gas sensor with catalytic reaction Pt electrode has been used to measure a series of gases. It has achieved long-term stable operation up to 600°C under experimental conditions [120]. The sensor has wide bandgap and is suitable for harsh environments. Casals *et al*. reported a gas sensor with a substrate of SiO_2-SiC. Pt catalytic gates and the $TaSi_x$ bonding layer were deposited on SiO_2-SiC substrate. Compared with SiC based sensors, this sensor had higher sensitivity in some gas detection such as CO and NO_2 [121].

2) Sensors Based on Nanomaterials

New nanomaterials such as carbon nanotubes, graphene, semiconducting metal oxide nanowires, nanorods, nanoribbons, nanoparticles, and some nanocomposites with special nanostructures can be used to fabricate gas sensors and humidity sensors. Nanomaterials have characteristics of high sensitivity, small volume and fast response and can be used for target gas detection, industrial process control, health monitoring, equipment humidity monitoring, etc. For instance, carbon nanotubes have abundant pore structure and large specific surface area, thus have strong adsorption capacity for some gas molecules. Thus, carbon nanotube-based sensors can be used to detect NH_3, CO, CO_2, ethanol, H_2, NO_2, Cl_2, ethylene and some organic vapors [122]–[126].

The main types of nano-sized multi-metal composite oxide include ABO_3, AB_2O_4, pyrochlore-structured $A_2B_2O_7$, etc. Metal composite oxides with certain structures have increased selectivity and sensitivity than regular compounds. For instance, by using sol-gel method, Wu *et al*. prepared $La_{0.75}Sr_{0.25}Cr_{0.5}Mn_{0.5}O_3$ perovskite-type composite oxide powder, which has linear response to concentrations of NO_2 [127].

3) Sensors Based on Polymer

Polymers are important materials in the field of sensors. Conductive polymers and their composites with other polymers which have active functional groups can be used in gas sensors [128]–[130]. Polymers can also be used to measure humidity value in industry or medicine [131], [132]. In these cases, polymers exhibit hydrophilicity. Recently, gas sensors based in polymer field-effect transistors are widely studied. They have applications in detecting NH_3, NO_2, H_2S, ethanol, etc [133]–[136].

4) Gas Sensing Micro-nano Sensor Array

Gas sensing micro-nano sensor arrays are fabricated by MEMS and nanoelectromechanical systems (NEMS) fabrication techniques. Based on input-output characteristics of fault-related gases, using advanced signal processing and pattern recognition algorithms, this kind of sensor can be used for detection of a single gas or gas mixtures with varied concentrations. Such gas/odor recognition systems based on integration of gas sensor array and multi-sensor information fusion technology are commonly referred to as E-noses.

Zampolli *et al*. constructed the E-nose for indoor detection of CO and NO_2. Temperature and humidity information was used for sensor calibration, and fuzzy logic is chosen as the pattern recognition algorithm. Results show the system was able to distinguish NO_2 with a volume fraction of 20×10^{-9} and CO with a volume fraction of 5×10^{-9} [137].

G. Motion Sensors

Motion sensors are sensors used to monitor movement of objects. Motion sensors include vibration sensors, acceleration sensors, gyroscopes, etc. At present, motion sensors have been widely used in smart phones, smart watches, sports bracelets and other devices to monitor the movement of the human body. For the ubiquitous power IoT, such sensors can be used in applications such as transmission line galloping monitoring and ice-covering monitoring.

1) Acceleration and Vibration Sensors

Acceleration sensors and vibration sensors are a type of sensors used to monitor changes in motion state of objects. Acceleration sensors and vibration sensors usually contain a mass. When motion state of the object changes, the mass will cause deformation inside the sensor. Therefore, such sensors can be designed based on deformation sensors. In addition to mass, typical acceleration or vibration sensors usually consist of dampers, elastic elements, sensitive elements and adaptive circuits. Common acceleration sensors and vibration sensors include capacitive sensors, piezoresistive sensors and piezoelectric sensors.

Capacitive acceleration sensors are generally designed as a movable structure. A typical capacitive acceleration sensor includes two sets of silicon fingers, one of which is fixed and the other moves with movement of the object. The two sets of silicon fingers are used as stationary and movable electrodes of the capacitor, respectively. By detecting change in capacitance between the electrodes, acceleration of the object can be measured. This type of sensor is mainly fabricated based on MEMS technology [138]–[140]. Acceleration sensors with double axis or triaxis have also been widely studied.

Piezoelectric acceleration sensors [141], [142] and piezoresistive acceleration sensors [143]–[145] convert acceleration of an object into internal deformation of the sensor, and then into a measurable signal. Take piezoelectric acceleration sensor as an example, the mass is in contact with a piezoelectric material. When an object moves, pressure between the mass and the piezoelectric material changes, causing charges of piezoelectric material to change. Acceleration can be measured by measuring change in current. This principle can also be used to measure angular acceleration [146].

In addition to the above principles, acceleration sensors also include force balance sensors, thermal convection sensors, resonance sensors, etc.

For vibration sensors, measurement can be performed using similar principles to acceleration sensors, such as capacitive sensors [147], [148] and piezoelectric sensors [149]. In addition, the optical principle can also be used to measure vibration [150].

2) Orientation Sensors

Gyroscope is the most common orientation sensor, which is used to sense and maintain direction of objects. The gyroscope is designed based on conservation of angular momentum. The gyroscope is mainly composed of a rotatable rotor located on the axis. Once the gyroscope starts to rotate, due to the angular momentum of the rotor, the gyroscope tends to resist change of direction. Gyroscopes are mostly used in navigation and positioning systems [151], [152].

Magnetometer is another type of orientation sensor. The magnetometer is essentially a magnetic field sensor used to measure the geomagnetic field. Orientation of the device is measured by the geomagnetic field. Unlike a gyroscope, a magnetometer can measure the angle between the device and geographic direction.

In addition, commonly used motion sensors also include speed sensors (including photoelectric and magnetoelectric sensors), angle sensors (mainly based on magnetoelectric effects), and obliquity sensors.

III. Applications of Sensor Data Acquired in UPIoT

Various types of data, when combined, can create even more opportunities for all the parties involved in the smart grid ecosystem to deliver and consume electricity in the best way possible [153]. In Fig. 14, diagram of the applications of sensor data from the ubiquitous power IOT is illustrated. By monitoring real-time status information of each key node and equipment of the power grid, through advanced control decision technology, real-time optimization and scheduling of the power grid can be realized, and optimal allocation and utilization efficiency of resources will be improved. Through rapid intelligent fault identification technology, it is possible to predict grid faults, quickly locate fault locations, determine cause of faults, and improve self-healing capability of the grid. Through online monitoring and diagnosis of equipment, life cycle management of grid equipment can be realized, and reliability and operation level of power supply can be improved. Through mass user information and power big data mining, an intelligent power interactive platform is formed to realize convenient interaction between power users and power grid, thus effectively balance power grid load, and explore value-added service potential of the power grid. Here we present some key applications of data analysis for power generation, transmission, distribution, and consumption with some emerging issues related to applications should be highlighted.

A key insight from Fig. 14 is a unified data platform is of crucial importance for various applications facilitated by the ubiquitous power IoT. Abstractions of applications and data assets accumulated in the power IoT need to be well-defined and scalable. Specifically, workload of adding new data sources or new types of data needs to be minimized. In addition, repetitive construction of data infrastructure for different applications should be avoided, which poses great challenges for operators of power systems. Ideally, all applications based on data within the ubiquitous power IoT would share a unified data platform. Business platforms can be further constructed based on the unified data platform. As the power system operates at various levels and has contrasting business models, multiple business platforms may exist in parallel. Applications can then be easily created and implemented with support of the data platform and business platforms.

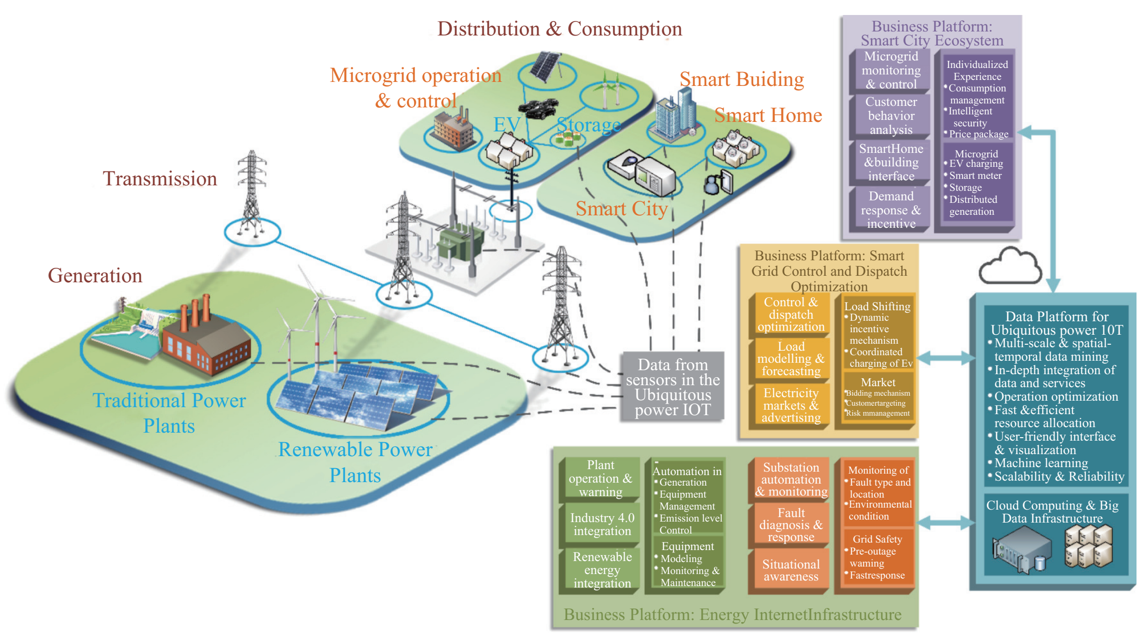

Fig. 14. An illustration of applications of sensor data in the ubiquitous power IOT. © [2021] IEEE. Reprinted, with permission, from [6].

A. State Awareness of Energy Internet and Equipment based on Sensor Data

1) Operation Safety Monitoring and Accident Warning of Power Plants

Operators are able to monitor operating status of equipment in power plants using pressure, temperature, vibration, voltage and current sensors. Ideally, data collected for the same type (or similar types) of equipment can be aggregated and analysed, revealing critical pre-fault patterns with high confidence. Service life of machines and devices can thus be maximized while minimizing expected cost of maintenance and shutdown (both planned or unplanned). In the meantime, company-level asset management systems based on data collection and analytics can also reduce labor and operation costs a great deal. Challenges for sensor deployment and data analytic methods for power plant management include:

a) The Integration of Domain Knowledge and Physical Models: It is often intractable to combine physical models of machines and devices in power plants with existing data analytic tools. In addition, it is important to take into consideration characteristics of the physical environment before deployment of WSNs in power plants [154].

b) Sharing Knowledge for Similar Equipment: With new types of equipment being manufactured and employed across the world constantly, it is desirable the knowledge mined out of data of certain equipment can be transferred to other equipment effectively.

2) Operation, Maintenance and Integration Management of Renewable Energy Sources

The operation, maintenance and integration management of wind farms and photovoltaic power stations relies heavily on monitoring of individual wind turbines and photovoltaic panels, as well as other observable quantities, which is well suited for WSNs. Another critical aspect of renewable energy integration is power forecasting. Sensors installed in or near wind farms, for instance, can collect data that help model the relationship between real-time weather conditions and generated power. When data of weather conditions and wind farm operation within a certain region can be integrated, prediction accuracy for wind farms within the whole region may be further improved. Modeling of solar irradiance and forecasting of solar power can also be improved by using data collected by WSNs [155]–[157]. Several issues related to renewable energy sources need to be addressed in the context of this paper:

a) The Maintenance of Equipment in Remote Areas: Wind turbines usually stand tens of meters from the ground (or even water), so it is very troublesome if a fault that requires manual maintenance occurs. Thus, it is necessary to conduct condition monitoring of wind turbines via WSNs [158]. In addition, it is desirable if knowledge of fault detection and diagnosis for wind turbines can be shared at the global level.

b) Distributed Learning Considering Spatio-temporal Characteristics: While it is well-acknowledged that spatio-temporal data of various sites can improve forecasting results of wind and solar power, operators of different sites may not be willing to share data they have collected. One way to compromise between data privacy and performance improvement is decomposing centralized analytical methods into distributed versions which require no data exchange [159]. In [160], a privacy-preserving distributed learning approach for wind power forecasting is proposed. The original large learning problem is solved iteratively in a decentralized manner where contracted agents and central agent collaboratively solve the same estimation problem while raw data is only used by contracted agents locally.

3) Online Monitoring of Substations and Power Equipment

There are many pieces of research on online monitoring of transformer, insulator, transformer, circuit breaker and lightning arrester in power transmission systems. In the framework of WSN, sensor data can not only reflect operating state of equipment, optimize strategies of regular outage and maintenance, but can also help establish probability models for equipment health status evolution under different system parameters or external conditions. Further, equipment design and manufacturing can also be upgraded with support of long-term operation data [161], [162].

Application of WSNs in remote system monitoring and equipment fault diagnostics is highlighted in [163], in which link quality measurements and experiments of WSNs in a 500-kV substation are reported, and a reliable metric for wireless link quality evaluation is proposed. Design considerations of WSNs for substation monitoring are discussed in [164]. A WSN design for mechanical failure detection in power transmission systems is proposed in [165].

For unmanned substations and remote power transmission systems, it is necessary to integrate camera data into the monitoring system. Augmented reality (AR) technologies can help visualize conditions of equipment being monitored by presenting multi-dimensional data (e.g., temperature, vibration level, and gas composition of power transformers). Convenient human-computer interaction is also critical for relevant personnel to complete monitoring tasks. Unmanned aerial vehicles (UAVs) can be used to monitor remote transmission systems by patrolling transmission lines automatically.

4) Fault Diagnosis in Smart Transmission Lines and Distribution Systems

Fault diagnosis of transmission and distribution systems is very important for long-term stable operation of power systems. Diagnosis of faults mainly contains fault detection, fault classification, and fault location [166]. High-precision broadband voltage and current sensors placed along transmission lines and at nodes of distribution systems are able to collect voltage and current waveforms containing critical information concerning fault type and location [167], [168]. Accurate fault classification and location greatly reduce time and effort spent on troubleshooting transmission and distribution systems. Reliability indices of systems can also be improved. An illustration of smart transmission lines based on WSNs is shown in Fig. 15. Smart power fittings based on advanced micro sensors are used as local nodes to monitor signals such as voltage and current of transmission lines, which act as peripheral nerves of smart transmission lines. Local node signals are processed through relay nodes for data processing such as edge computing, data compression, and

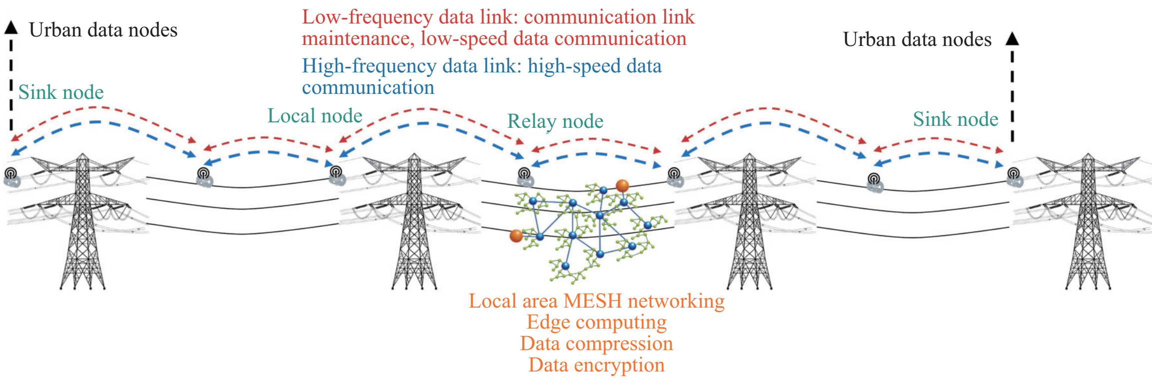

Fig. 15. An illustration of smart transmission lines based on WSN.

data encryption. Processed data is imported into the master station through the sink node for data center processing. Based on WSNs, panoramic information sensing platform can be built, realizing real-time statue evaluation and prediction and fault and risk warning of transmission and distribution lines. This structure can improve flexibility and integrity of installation of sensing equipment.

5) Power System Situational Awareness

Data collected by WSNs can help the power system analyze its status. Power system operators also hope to be able to predict possible instability events or accidents. In addition, the system should also have the ability to recover timely after accidents. Comprehensive tools for data aggregation and presentation will help operators respond to the specific situation properly and make appropriate decisions.

Developments of a WAMS named FNET/GridEye is introduced in [169]. More specifically, applications deployed on the system include real-time visualization of measured data, recognition, and location of disturbances, detection and modal analysis of inter-area oscillation, detection of islanding and off-grid, etc. A number of non-real-time applications are also supported. In order to support more real-time applications such as power system dynamic response estimation, as well as new data analytics algorithms, the distributed version of FNET/GridEye is developed [170]. Concretely, real-time applications (tier 1) are executed on data servers where synchrophasor measurements are collected. Near-real-time applications (tier 2) are completed in the analytics cluster containing a series of computation nodes. Further, offline applications such as big data analytics can be implemented by the analytics cluster when no near-real-time applications are being processed.

A data-driven distributed analytics and control platform for smart grids with hierarchical structures is proposed in [171]. The proposed framework can easily be applied to natural electrical hierarchies (e.g., the substation-feeder-distribution transformer-customer hierarchy) to complete data management and control tasks.

B. Smart Grid Control and Dispatch Optimization Based on Sensor Data

1) Smart Control Towards Increased Stability and Resilience

A more transparent power grid is not only more observable but also more controllable. Compared with traditional power system control systems, control agents of future smart grids need to be able to process real-time heterogeneous signals collected by WSNs with certain hierarchies, combine data-driven analytics methods with the physical mechanism of power systems, take into consideration risks both globally and locally, and guarantee results of control are optimized in the long run. In the next section, we will discuss how reinforcement learning can be applied to control of power systems.

2) Management of the Two-way Flows of Information and Energy

Two-way flows of both energy and information are critical features of future smart grids. A stable and efficient cyber-physical system is indispensable for transformation from one energy source to another and role exchange between traditional energy suppliers and receivers. As the primary provider of information, WSNs are crucial for two-way flow of energy and information.

3) Load Monitoring, Prediction, and Regulation

Difficulties of predicting and regulating energy consumption are increased under the premise that various types of energy sources can be converted to one another and a large number of distributed energy resources and energy storage systems are interconnected [172]–[174]. For example, power of a DG system is often highly stochastic and hard to be precisely predicted. Generated power can be used directly in situ, fed into the energy storage system (electric vehicle (EV) batteries can also be considered as energy storage devices in some cases), or delivered to the power grid. Thus, it is necessary to monitor all relevant parts of the system and take all collected data into consideration. When large amounts of data and models are accumulated, accurate prediction and efficient regulation of loads will also be easier to achieve.

4) Dynamic Operation of Electricity Markets

High penetration of renewable energy, involvement of energy storage systems and demand response programs pose challenges for operation of electricity markets, especially ones with competitive mechanisms. Advanced data analytic tools are required to account for randomness and complexity brought about by all parties of the markets, so day-ahead and real-time prices can be properly proposed, and all parties can take what they need in an optimized manner. Data collected by the WSNs and high-performance data analytics platform can provide huge support for operators of electricity markets.

C. Intelligent Electricity Consumption Based on Sensor Data

1) Monitoring and Management of Microgrids

Microgrids in the smart grid consist of distributed photovoltaic and wind power generation systems, power storage systems, cold and heat storage systems, EVs and different types of loads [175]. Monitoring and management of these elements can be integrated into intelligent microgrid monitoring and management system facilitated by WSNs [176].

2) Integration of Wireless Sensor Networks into the Industry 4.0 Framework Towards Intelligent Manufacturing

The process of industrial production under the framework of industry 4.0 is facilitated by cyber-physical production system. The concept of the intelligent factory would have profound impacts on manufacturing enterprises, power plants, and energy system as a whole. M2 M communication enabled by WSNs with sensors installed on machines, products, and conveyors can increase global efficiency in a self-organized manner [177]. Collaborative communication can start from sensor level and reach all the way to enterprise level and thus end-to-end digital integration becomes possible [178].

3) Management of the Smart Home System

A safe, comfortable and pleasant living experience can be guaranteed by a smart-home system featuring, among others, temperature, gas, smoke, infrared and pressure sensors that are properly installed in the house. Under management of the smart-home system, household appliances, renewable energy generation devices, energy storage devices, EVs, heating devices, as well as intelligent security system can be integrated into a unified framework. In [179], a smart lighting control system based on WSNs is proposed. More than 40% of energy used for lighting can be saved when the proposed system is used. Apart from meeting some default standards, the smart home system should also adapt to residents living inside the home. Not only can residents interact with appliances and devices in and out of the house anytime and anywhere via computers [180], smartphones [181], voice or even hand gestures, but behaviour patterns (e.g., energy consumption or movement patterns) of individuals can also be recorded and analyzed in order to improve living experience [181], [182].

4) Electricity Consumption Behaviour Modeling and Analysis

One of the key prerequisites for effective load forecasting and demand response is having a good understanding of consumer behaviour [183]. Thus, in order to understand and abstract end-user behaviour based on smart meter data, researchers have been working on various methods for load profiling and clustering. Here, we mainly focus on how the smart meter data is processed and used. Challenges faced by load profiling and clustering with rapid growing data volume and application requirements is listed as follows:

a) The Clustering Results Need to be More Effective and Explicable: Although a variety of clustering methods have been implemented and evaluated on different datasets, simply clustering daily load curves does not directly yield load patterns with high representativeness, as is pointed out in [184]. Firstly, the centroids (or means) of the clusters may not represent all cluster members very well due to the high dimensionality and stochasticity of residential daily load curves. Further, high-dimensional data points of the daily load curves are oftentimes hard to be explicitly separated. Instead of finding existing clusters with closely aggregated data points (or with distinctly high density), clustering algorithms may only divide data points into several clusters so the objective function reaches optimum. As a consequence, a lot of data points close to cluster boundaries may be assigned randomly. The same problem may still exist even if some feature extraction process is implemented or a longer period of time (rather than only a day) is considered. Thus, it is of great importance to find some features that can help distinctly separate customers, which would greatly facilitate further applications of such clustering results. In addition, as a large number of smart meters are constantly being installed and number of users changes rapidly, scalability of the analytic tools must be ensured.

b) The Way in Which High-dimensional Raw Data is Processed and Aggregated Needs Further Study and Discussion: In [185], authors use energy consumption of all consumers in the system at a given time instant as a data point, which means dimensionality of data points can remain constant given a fixed number of consumers. Nevertheless, an appropriate method for single-household load pattern representation and characterization is needed, considering each residential user as a data point assigned to a group is far from enough for applications such as household energy management. Analysis of end-user behaviour based on load profiling and clustering may also be combined with methods of appliance-level analysis such as non-intrusive load monitoring (NILM).

5) Realization of Demand Response Mechanism

It is necessary to consider both the target of the response and characteristics of users, so the most appropriate users can be selected and encouraged to participate in the response, thus enhancing the response result, as well as user experience [186]. The above-mentioned electricity consumption behaviour analysis and smart home system are critical to realization of demand response projects.

IV. Conclusion

The Ubiquitous power internet of things (UPIoT) is an important technology for innovation of power and energy industries. It is the basis for information flow in the energy Internet. Advanced sensor technology, network and communication technology, big data and artificial intelligence technology are key technologies for building UPIoT.

Advanced sensors such as current sensors, voltage sensors, and temperature sensors help to collect physical information data of different nodes of the system. Performance of sensors can be improved effectively with advances in materials development and processing technologies. Wireless sensor network

(WSNs) realizes interconnection of information of various parts of the system. By coordinating edge computing and cloud computing, using advanced communication methods, system data transfer and processing efficiency can be improved. Collected data has important applications in network operation monitoring, new energy management, and development of smart devices.

At present, technologies of UPIoT still need to be improved. Performance of various sensors, information transmission methods and information processing methods still need further research. UPIoT will drive development of sensors, information communication, computer technology and other industries. Furthermore, UPIoT can provide open and efficient data exchange and management platform to connect all aspects of the power system. It will promote development of many new technologies and new businesses, and finally form an industrial chain based on UPIoT.

References

[1] A. Q. Huang, M. L. Crow, G. T. Heydt, J. P. Zheng, and S. J. Dale, "The future renewable electric energy delivery and management (FREEDM) system: the energy internet," *Proceedings of the IEEE*, vol. 99, no. 1, pp. 133–148, Jan. 2011.

[2] S. Y. Chen, S. F. Song, L. X. Li, and J. Shen, "Survey on smart grid technology," *Power System Technology*, vol. 33, no. 8, pp. 1–7, 2009.

[3] H. Farhangi, "The path of the smart grid," *IEEE Power and Energy Magazine*, vol. 8, no. 1, pp. 18–28, Jan./Feb. 2010.

[4] X. Fang, S. Misra, G. L. Xue, and D. J. Yang, "Smart grid — the new and improved power grid: a survey," *IEEE Communications Surveys & Tutorials*, vol. 14, no. 4, pp. 944–980, 2011.

[5] Q. Y. Chen, "Research on implementation strategy of ubiquitous power internet of things," *Power Generation Technology*, vol. 40, no. 2, pp. 99–106, Apr. 2019.

[6] Z. F. Han, F. Xue, J. Hu, and J. L. He, "Micro electric field sensors: principles and applications," *IEEE Industrial Electronics Magazine*, vol. 15, no. 4, pp. 35–42, Dec. 2021.

[7] Y. Ouyang, J. L. He, J. Hu, G. Zhao, Z. X. Wang, and S. X. Wang, "Contactless current sensors based on magnetic tunnel junction for smart grid applications," *IEEE Transactions on Magnetics*, vol. 51, no. 11, pp. 4004904, Nov. 2015.

[8] V. C. Gungor, D. Sahin, T. Kocak, S. Ergut, C. Buccella, C. Cecati, and G. P. Hancke, "Smart grid technologies: communication technologies and standards," *IEEE Transactions on Industrial Informatics*, vol. 7, no. 4, pp. 529–539, Nov. 2011.

[9] J. C. Han, J. Hu, Y. Yang, Z. X. Wang, S. X. Wang, and J. L. He, "A nonintrusive power supply design for self-powered sensor networks in the smart grid by scavenging energy from AC power line," *IEEE Transactions on Industrial Electronics*, vol. 62, no. 7, pp. 4398–4407, Jul. 2015.

[10] A. Ukil, H. Braendle, and P. Krippner, "Distributed temperature sensing: review of technology and applications," *IEEE Sensors Journal*, vol. 12, no. 5, pp. 885–892, May 2012.

[11] A. Chatterjee, P. Bhattacharjee, N. K. Roy, and P. Kumbhakar, "Usage of nanotechnology based gas sensor for health assessment and maintenance of transformers by DGA method," *International Journal of Electrical Power & Energy Systems*, vol. 45, no. 1, pp. 137–141, Feb. 2013.

[12] K. Schroeder, W. Ecke, J. Apitz, E. Lembke, and G. Lenschow, "A fibre Bragg grating sensor system monitors operational load in a wind turbine rotor blade," *Measurement Science and Technology*, vol. 17, no. 5, pp. 1167–1172, Apr. 2006.

[13] C. C., Xiao, L. Y. Zhao, T. Asada, W. G. Odendaal, and J. D. van Wyk, "An overview of integratable current sensor technologies," in *Proceedings of the 38th IAS Annual Meeting on Conference Record of the Industry Applications Conference*, 2003, pp. 1251–1258.

[14] P. Ripka, "Electric current sensors: a review," *Measurement Science and Technology*, vol. 21, no. 11, pp. 112001, Sep. 2010.

[15] S. Ziegler, R. C. Woodward, H. H. C. Iu, and L. J. Borle, "Current sensing techniques: a review," *IEEE Sensors Journal*, vol. 9, no. 4, pp. 354–376, Apr. 2009.

[16] B. Voljc, M. Lindic, and R. Lapuh, "Direct measurement of AC current by measuring the voltage drop on the coaxial current shunt," *IEEE Transactions on Instrumentation and Measurement*, vol. 58, no. 4, pp. 863–867, Apr. 2009.

[17] P. S. Filipski and M. Boecker, "AC-DC current shunts and system for extended current and frequency ranges," *IEEE Transactions on Instrumentation and Measurement*, vol. 55, no. 4, pp. 1222–1227, Aug. 2006.

[18] K. Lind, T. Sørsdal, and H. Slinde, " Design, modeling, and verification of high-performance AC-DC current shunts from inexpensive components," *IEEE Transactions on Instrumentation and Measurement*, vol. 57, no. 1, pp. 176–181, Jan. 2008.

[19] N. Locci and C. Muscas, "A digital compensation method for improving current transformer accuracy," *IEEE Transactions on Power Delivery*, vol. 15, no. 4, pp. 1104–1109, Oct. 2000.

[20] Q. Chen, H. B. Li, M. M. Zhang, and Y. B. Liu, "Design and characteristics of two Rogowski coils based on printed circuit board," *IEEE Transactions on Instrumentation and Measurement*, vol. 55, no. 3, pp. 939–943, Jun. 2006.

[21] W. Stygar and G. Gerdin, "High frequency rogowski coil response characteristics," *IEEE Transactions on Plasma Science*, vol. 10, no. 1, pp. 40–44, Mar. 1982.

[22] D. G. Pellinen, M. S. Di Capua, S. E. Sampayan, H. Gerbracht, and M. Wang, "Rogowski coil for measuring fast, high-level pulsed currents," *Review of Scientific Instruments*, vol. 51, no. 11, pp. 1535–1540, Nov. 1980.

[23] J. E. Lenz, "A review of magnetic sensors," *Proceedings of the IEEE*, vol. 78, no. 6, pp. 973–989, Jun. 1990.

[24] J. Lenz and S. Edelstein, "Magnetic sensors and their applications," *IEEE Sensors Journal*, vol. 6, no. 3, pp. 631–649, Jun. 2006.

[25] A. Roux, O. Le contel, C. Coillot, A. Bouabdellah, B. de la Porte, D. Alison, S. Ruocco, and M. C. Vassal, "The search coil magnetometer for THEMIS," *Space Science Reviews*, vol. 141, no. 1–4, pp. 265–275, Nov. 2008.

[26] H. C. Séran and P. Fergeau, "An optimized low-frequency three-axis search coil magnetometer for space research," *Review of Scientific Instruments*, vol. 76, no. 4, pp. 044502, Apr. 2005.

[27] F. Primdahl, "The fluxgate magnetometer," *Journal of Physics E: Scientific Instruments*, vol. 12, no. 4, pp. 241–253, Apr. 1979.

[28] P. Ripka, "Advances in fluxgate sensors," *Sensors and Actuators A: Physical*, vol. 106, no. 1–3, pp. 8–14, Sep. 2003.

[29] M. H. Acuna and C. J. Pellerin, "A miniature two-axis fluxgate magnetometer," *IEEE Transactions on Geoscience Electronics*, vol. 7, no. 4, pp. 252–260, Oct. 1969.

[30] L. Sileo, M. T. Todaro, V. Tasco, M. De Vittorio, and A. Passaseo, "Fully integrated three-axis Hall magnetic sensor based on micromachined structures," *Microelectronic Engineering*, vol. 87, no. 5–8, pp. 1217–1219, May/Aug. 2010.

[31] P. Leroy, C. Coillot, V. Mosser, A. Roux, and G. Chanteur, "An ac/dc magnetometer for space missions: improvement of a Hall sensor by the magnetic flux concentration of the magnetic core of a searchcoil," *Sensors and Actuators A: Physical*, vol. 142, no. 2, pp. 503–510, Apr. 2008.

[32] Y. Ouyang, J. Hu, J. L. He, G. Zhao, F. Xue, Z. X. Wang, S. X. Wang, Z. Y. Yuan, and Z. J. Ding, "Modeling the frequency dependence of packaged linear magnetoresisitive sensors based on MTJ," *IEEE Transactions on Magnetics*, vol. 50, no. 11, pp. 4006404, Nov. 2014.

[33] Y. Ouyang, J. L. He, J. Hu, G. Zhao, Z. X. Wang, and S. X. Wang, "Prediction and optimization of linearity of MTJ magnetic sensors based on single-domain model," *IEEE Transactions on Magnetics*, vol. 51, no. 11, pp. 4004204, Nov. 2015.

[34] D. A. Thompson, L. Romankiw, and A. Mayadas, "Thin film magnetoresistors in memory, storage, and related applications," *IEEE Transactions on Magnetics*, vol. 11, no. 4, pp. 1039–1050, Jul. 1975.

[35] R. Schad, C. D. Potter, P. Beliën, G. Verbanck, V. V. Moshchalkov, and Y. Bruynseraede, "Giant magnetoresistance in Fe/Cr superlattices with very thin Fe layers," *Applied Physics Letters*, vol. 64, no. 25, pp. 3500–3502, Jun. 1994.

[36] M. Löhndorf, T. Duenas, M. Tewes, E. Quandt, M. Rührig, and J. Wecker, "Highly sensitive strain sensors based on magnetic tunneling junctions," *Applied Physics Letters*, vol. 81, no. 2, pp. 313–315, Jul. 2002.

[37] W. P. Jr. Pratt, S. F. Lee, J. M. Slaughter, R. Loloee, P. A. Schroeder, and J. Bas, "Perpendicular giant magnetoresistances of Ag/Co multilayers," *Physical Review Letters*, vol. 66, no. 23, pp. 3060–3063, Jun. 1991.

[38] W. J. Tabor and F. S. Chen, "Electromagnetic propagation through materials possessing both faraday rotation and birefringence: experiments with ytterbium orthoferrite," *Journal of Applied Physics*, vol. 40, no. 7, pp. 2760–2765, Jun. 1969.

[39] D. Budker, D. F. Kimball, S. M. Rochester, V. V. Yashchuk, and M. Zolotorev, "Sensitive magnetometry based on nonlinear magneto-optical rotation," *Physical Review A*, vol. 62, no. 4, pp. 043403, Sep. 2000.

[40] D. M. Dagenais, F. Bucholtz, K. P. Koo, and A. Dandridge, "Detection of low-frequency magnetic signals in a magnetostrictive fiber-optic sensor with suppressed residual signal," *Journal of Lightwave Technology*, vol. 7, no. 6, pp. 881–887, Jun. 1989.

[41] F. Bucholtz, D. M. Dagenais, K. P. Koo, and S. T. Vohra, "Recent developments in fiber optic magnetostrictive sensors," in *Proceedings of SPIE 1367*, *Fiber Optic and Laser Sensors VIII*, 1991.

[42] E. M. Purcell, H. C. Torrey, and R. V. Pound, "Resonance absorption by nuclear magnetic moments in a solid," *Physical Review*, vol. 69, no. 1–2, pp. 37–38, Jan. 1946.

[43] A. Dutta, and C. N. Archie, "High field nuclear magnetometer," *Review of Scientific Instruments*, vol. 58, no. 4, pp. 628–631, Apr. 1987.

[44] J. Magnusson, C. Djurberg, P. Granberg, and P. Nordblad, "A low field superconducting quantum interference device magnetometer for dynamic measurements," *Review of Scientific Instruments*, vol. 68, no. 10, pp. 3761–3765, Oct. 1997.

[45] R. H. Koch, J. Z. Sun, V. Foglietti, and W. J. Gallagher, "Flux dam, a method to reduce extra low frequency noise when a superconducting magnetometer is exposed to a magnetic field," *Applied Physics Letters*, vol. 67, no. 5, pp. 709–711, Jul. 1995.

[46] Y. Ouyang, J. L. He, J. Hu, and S. X. Wang, "A current sensor based on the giant magnetoresistance effect: design and potential smart grid applications," *Sensors*, vol. 12, no. 11, pp. 15520–15541, Nov. 2012.

[47] G. Zhao, J. Hu, Y. Ouyang, J. L. He, S. X. Wang, and Z. Y. Yuan, "Mobile ions generated by external direct current electric field influence direct current measurement of giant magnetoresistance current sensors," *Journal of Applied Physics*, vol. 117, no. 17, pp. 17A307, May 2015.

[48] Y. Ouyang, Z. X. Wang, G. Zhao, J. Hu, S. J. Ji, J. L. He, and S. X. Wang, "Current sensors based on GMR effect for smart grid applications," *Sensors and Actuators A: Physical*, vol. 294, pp. 8–16, Aug. 2019.

[49] G. Zhao, J. Hu, Y. Ouyang, W. Z. Chang, Z. X. Wang, S. X. Wang, J. L. He, and J. G. Bi, "Novel method for magnetic field vector measurement based on dual-axial tunneling magnetoresistive sensors," *IEEE Transactions on Magnetics*, vol. 53, no. 8, pp. 4400306, Aug. 2017.

[50] G. Zhao, J. Hu, S. Zhao, Z. X. Wang, S. X. Shan, Wang, and J. L. He, "Current reconstruction of bundle conductors based on tunneling magnetoresistive sensors," *IEEE Transactions on Magnetics*, vol. 53, no. 11, pp. 4004005, Nov. 2017.

[51] C. Daniel Oancea and C. Dinu, "LEM transducers interface for voltage and current monitoring," *2015 9th International Symposium on Advanced Topics in Electrical Engineering (ATEE)*, Bucharest, Romania, 2015, pp. 949–952

[52] P. Skeath, C. H. Bulmer, S. C. Hiser, and W. K. Burns, "Novel electrostatic mechanism in the thermal instability of z-cut $LiNbO_3$ interferometers," *Applied Physics Letters*, vol. 49, no. 19, pp. 1221–1223, Nov. 1986.

[53] C. H. Bulmer, W. K. Burns, and S. C. Hiser, "Pyroelectric effects in $LiNbO_3$ channel-waveguide devices," *Applied Physics Letters*, vol. 48, no. 16, pp. 1036–1038, Apr. 1986.

[54] M. M. Howerton, C. H. Bulmer, and W. K. Burns, "Effect of intrinsic phase mismatch on linear modulator performance of the 1*2 directional coupler and Mach-Zehnder interferometer," *Journal of Lightwave Technology*, vol. 8, no. 8, pp. 1177–1186, Aug. 1990.

[55] C. H. Bulmer, W. K. Burn, and A. S. Greenblatt, "Phase tuning by laser ablation of $LiNbO_3$ interferometric modulators to optimum linearity," *IEEE Photonics Technology Letters*, vol. 3, no. 6, pp. 510–512, Jun. 1991.

[56] A. S. Greenblatt, C. H. Bulmer, R. P. Moeller, and W. K. Burns, "Thermal stability of bias point of packaged linear modulators in lithium niobate," *Journal of Lightwave Technology*, vol. 13, no. 12, pp. 2314–2319, Dec. 1995.

[57] K. Tajima, R. Kobayashi, N. Kuwabara, and M. Tokuda, "Frequency bandwidth improvement of electric field sensor using optical modulator by resistively loaded element," *Electrical Engineering in Japan*, vol. 123, no. 4, pp. 25–33, Jun. 1998.

[58] R. Kobayashi, K. Tajima, N. Kuwabara, and M. Tokuda, "Improvement of frequency characteristics of electric field sensor using Mach-Zehnder interferometer," *Electronics and Communications in Japan* (*Part I: Communications*), vol. 83, no. 11, pp. 76–84, Nov. 2000.

[59] K. Tajima, R. Kobayashi, N. Kuwabara, and M. Tokuda, "Development of optical isotropic E-field sensor operating more than 10 GHz using Mach-Zehnder interferometer," *IEICE Transactions on Electronics*, vol. E85-C, no. 4, pp. 961–968, Apr. 2002.

[60] T. Meier, K. Kostrzcewa, B. Schüppert, and K. Petermann, "Electro-optical E-field sensor with optimised electrode structure," *Electronics Letters*, vol. 28, no. 14, pp. 1327–1329, Jul. 1992.

[61] T. Meier, C. Kostrzewa, K. Petermann, and B. Schuppert, "Integrated optical E-field probes with segmented modulator electrodes," *Journal of Lightwave Technology*, vol. 12, no. 8, pp. 1497–1503, Aug. 1994.

[62] M. Schwerdt, J. Berger, B. Schuppert, and K. Petermann, "Integrated optical E-field sensors with a balanced detection scheme," *IEEE Transactions on Electromagnetic Compatibility*, vol. 39, no. 4, pp. 386–390, Nov. 1997.

[63] J. Berger, D. Pouhè, G. Mönich, H. Fähling, P. Wust, and K. Petermann, "Calibration cell for E-field sensors in water environment," *Electronics Letters*, vol. 35, no. 16, pp. 1317–1318, Aug. 1999.

[64] R. Zeng, B. Wang, Z. Q. Yu, and W. Y. Chen, "Design and application of an integrated electro-optic sensor for intensive electric field measurement," *IEEE Transactions on Dielectrics and Electrical Insulation*, vol. 18, no. 1, pp. 312–319, Feb. 2011.

[65] R. Zeng, J. J. Yu, B. Wang, B. Niu, and Y. Hua, "Study of an integrated optical sensor with mono-shielding electrode for intense transient E-field measurement," *Measurement*, vol. 50, pp. 356–362, Apr. 2014.

[66] M. M. Howerton, C. H. Bulmer, and W. K. Burns, "Linear 1×2 directional coupler for electromagnetic field detection," *Applied Physics Letters*, vol. 55, no. 22, pp. 1850–1852, May 1988.

[67] R. Zeng, B. Wang, Z. Q. Yu, B. Niu, and Y. Hua, "Integrated optical E-field sensor based on balanced Mach–Zehnder interferometer," *Optical Engineering*, vol. 50, no. 11, pp. 114404, Nov. 2011.

[68] N. A. F. Jaeger, "Integrated optics pockels cell voltage sensor," U.S. Patent 5029273, Jul. 2, 1991.

[69] T. Takahashi, K. Hidaka, and T. Kouno, "New optical-waveguide pockels sensor for measuring electric fields," *Japanese Journal of Applied Physics*, vol. 35, no. 2R, pp. 767–771, Feb. 1996.

[70] T. Takahashi, "Electric field measurement just beneath a surface discharge by optical-waveguide pockels sensors," *Electrical Engineering in Japan*, vol. 145, no. 2, pp. 28–34, Nov. 2003.

[71] R. Zeng, B. Wang, B. Niu, and Z. Q. Yu, "Development and application of integrated optical sensors for intense E-field measurement," *Sensors*, vol. 12, no. 8, pp. 11406–11434, Aug. 2012.

[72] F. Xue, J. Hu, Y. Guo, G. W. Han, Y. Ouyang, S. X. Wang, and J. L. He, "Piezoelectric-piezoresistive coupling MEMS sensors for measurement of electric fields of broad bandwidth and large dynamic range," *IEEE Transactions on Industrial Electronics*, vol. 67, no. 1, pp. 551–559, Jan. 2020.

[73] F. Xue, J. Hu, S. X. Wang, and J. L. He, "Electric field sensor based on piezoelectric bending effect for wide range measurement," *IEEE Transactions on Industrial Electronics*, vol. 62, no. 9, pp. 5730–5737, Sep. 2015.

[74] Z. F. Han, F. Xue, G. Z. Yang, Z. Q. Yu, J. Hu, and J. L. He, "Micro-cantilever capacitive sensor for high-resolution measurement of electric fields," *IEEE Sensors Journal*, vol. 21, no. 4, pp. 4317–4324, Feb. 2021.

[75] A. Dante, R. M. Bacurau, A. W. Spengler, E. C. Ferreira, and J. A. S. Dias, "A temperature-independent interrogation technique for FBG sensors using monolithic multilayer piezoelectric actuators," *IEEE Transactions on Instrumentation and Measurement*, vol. 65, no. 11, pp. 2476–2484, Nov. 2016.

[76] R. C. Allil and M. M. Werneck, "Optical high-voltage sensor based on fiber Bragg grating and PZT piezoelectric ceramics," *IEEE Transactions on Instrumentation and Measurement*, vol. 60, no. 6, pp. 2118–2125, Jun. 2011.

[77] G. Fusiek and P. Niewczas, "Laboratory investigation of an intensiometric dual FBG-based hybrid voltage sensor," in *Proceedings of SPIE 9634*, *24th International Conference on Optical Fibre Sensors*, 2015, pp. 96341H.

[78] Q. Yang, Y. X. He, S. P. Sun, M. D. Luo, and R. Han, "An optical fiber Bragg grating and piezoelectric ceramic voltage sensor," *Review of Scientific Instruments*, vol. 88, no. 10, pp. 105005, Oct. 2017.

[79] P. S. Riehl, K. L. Scott, R. S. Muller, R. T. Howe, and J. A. Yasaitis, "Electrostatic charge and field sensors based on micromechanical resonators," *Journal of Microelectromechanical Systems*, vol. 12, no. 5, pp. 577–589, Oct. 2003.

[80] C. R. Peng, X. X. Chen, C. Ye, H. Tao, G. P. Cui, Q. Bai, S. F. Chen, and S. H. Xia, "Design and testing of a micromechanical

resonant electrostatic field sensor," *Journal of Micromechanics and Microengineering*, vol. 16, no. 5, pp. 914–919, Mar. 2006.

[81] C. R. Peng, P. F. Yang, X. Guo, H. Y. Zhang, and S. H. Xia, "Measuring atmospheric electric field using novel micromachined sensor," in *Proceedings of the 6th IEEE International Conference on Nano/Micro Engineered and Molecular Systems*, 2011, pp. 417–420.

[82] Y. Mou, Z. Yu, K. Huang, Q. Ma, R. Zeng, and Z.Wang, "Research on a novel MEMS sensor for spatial DC electric field measurements in an ion flows field," *Sensors*, vol.18, no.6, 1740, 2018.

[83] K. T. Huang, Z. Q. Yu, Z. Y. Gao, R. Zeng, M. Li, and L. Liu, "The charging process on sensor's shell in ion flow field and its influence towards electric field near HVDC lines," in *Proceedings of 2016 Asia-Pacific International Symposium on Electromagnetic Compatibility*, 2016, pp. 540–543.

[84] Q. Ma, K. T. Huang, Z. Q. Yu, and Z. Y. Wang, "A MEMS-based electric field sensor for measurement of high-voltage DC synthetic fields in air," *IEEE Sensors Journal*, vol. 17, no. 23, pp. 7866–7876, Dec. 2017.

[85] A. Kainz, H. Steiner, J. Schalko, A. Jachimowicz, F. Kohl, M. Stifter, R. Beigelbeck, F. Keplinger, and W. Hortschitz, "Distortion-free measurement of electric field strength with a MEMS sensor," *Nature Electronics*, vol. 1, no. 1, pp. 68–73, Jan. 2018.

[86] Z. F. Han, F. Xue, J. Hu, and J. L. He, "Trampoline-shaped micro electric-field sensor for AC/DC high electric field measurement," *IEEE Transactions on Industrial Electronics*, vol. 69, no. 12, pp. 13791–13798, Dec. 2022.

[87] Z. F. Han, J. Hu, L. C. Li, and J. L. He, "Micro-cantilever electric field sensor driven by electrostatic force," *Engineering*, vol. 24, pp. 184–191. May 2023.

[88] X. Wu. A sensitivity-enhanced electric field sensor with electrostatic field bias. In: 2017 IEEE Sensors, IEEE.

[89] T. Chen, C. Shafai, A. Rajapakse, J. S. H. Liyanage, and T. D. Neusitzer, "Micromachined ac/dc electric field sensor with modulated sensitivity," *Sensors and Actuators A: Physical*, vol. 245, pp. 76–84, Jul. 2016.

[90] C. S. Li and W. Q. Wang, "Review of optical voltage sensor based on electroluminescent effect," *Chinese Optics*, vol. 9, no. 1, pp. 30–40, Feb. 2016.

[91] T. Mizuno, Y. S. Liu, W. Shionoya, M. Okada, K. Yasuoka, S. Ishii, A. Yokoyama, and H. Miyata, "Electroluminescence from surface layer of insulating polymer under ac voltage application," *IEEE Transactions on Dielectrics and Electrical Insulation*, vol. 5, no. 6, pp. 903–908, Dec. 1998.

[92] H. Takeda, T. Shimada, Y. Katsuyama, and T. Shiosaki, "Fabrication and operation limit of lead-free PTCR ceramics using $BaTiO_3$-$(Bi_{1/2}Na_{1/2})TiO_3$ system," *Journal of Electroceramics*, vol. 22, no. 1–3, pp. 263–269, Feb. 2009.

[93] H. Takeda, H. Harinaka, T. Shiosaki, M. A. Zubair, C. Leach, R. Freer, T. Hoshina, and T. Tsurumi, "Fabrication and positive temperature coefficient of resistivity properties of semiconducting ceramics based on the $BaTiO_3$-$(Bi_{1/2}K_{1/2})TiO_3$ system," *Journal of the European Ceramic Society*, vol. 30, no. 2, pp. 555–559, Jan. 2010.

[94] S. L. Leng, G. R. Li, L. Y. Zheng, T. B. Wang, and Q. R. Yin, "Synthesis of Y-doped $BaTiO_3$-$(Bi_{1/2}K_{1/2})TiO_3$ lead-free positive temperature coefficient of resistivity ceramics and their PTC effects," *Journal of the American Ceramic Society*, vol. 92, no. 11, pp. 2772–2775, Nov. 2009.

[95] Y. Y. Li, G. R. Li, T. B. Wang, L. Y. Zheng, S. L. Leng, and Q. R. Yin, "Effects of niobium-doping on the structure and electrical properties of (Ba, Bi, Na)TiO_3-based PTCR ceramics," *Journal of Inorganic Materials*, vol. 24, no. 2, pp. 374–378, Mar. 2009.

[96] A. Hartog, "A distributed temperature sensor based on liquid-core optical fibers," *Journal of Lightwave Technology*, vol. 1, no. 3, pp. 498–509, Sep. 1983.

[97] A. H. Hartog, A. P. Leach, and M. P. Gold, "Distributed temperature sensing in solid-core fibres," *Electronics Letters*, vol. 21, no. 23, pp. 1061–1062, Nov. 1985.

[98] W. Ma, M. Ma, H. Wang, Z. Zhang, R. Zhang and J. Wang, "Shading Fault Detection Method for Household Photovoltaic Power Stations Based on Inherent Characteristics of Monthly String Current Data Mapping," *CSEE Journal of Power and Energy Systems*, vol. 9, no. 4, pp. 1370–1382, Jul. 2023.

[99] T. Horiguchi and M. Tateda, "Optical-fiber-attenuation investigation using stimulated Brillouin scattering between a pulse and a continuous wave," *Optics Letters*, vol. 14, no. 8, pp. 408–410, Apr. 1989.

[100] M. A. Soto, X. Angulo-Vinuesa, S. Martin-Lopez, S. H. Chin, J. D. Ania-Castanon, P. Corredera, E. Rochat, M. Gonzalez-Herraez, and L. Thevenaz, "Extending the real remoteness of long-range Brillouin optical time-domain fiber analyzers," *Journal of Lightwave Technology*, vol. 32, no. 1, pp. 152–162, Jan. 2014.

[101] Y. K. Dong, L. Chen, and X. Y. Bao, "Extending the sensing range of Brillouin optical time-domain analysis combining frequency-division multiplexing and in-line EDFAs," *Journal of Lightwave Technology*, vol. 30, no. 8, pp. 1161–1167, Apr. 2012.

[102] Y. K. Dong, H. Y. Zhang, L. Chen, and X. Y. Bao, "2 cm spatial-resolution and 2 km range Brillouin optical fiber sensor using a transient differential pulse pair," *Applied Optics*, vol. 51, no. 9, pp. 1229–1235, Mar. 2012.

[103] W. W. Zou, Z. Y. He, and K. Hotate, "Complete discrimination of strain and temperature using Brillouin frequency shift and birefringence in a polarization-maintaining fiber," *Optics Express*, vol. 17, no. 3, pp. 1248–1255, Feb. 2009.

[104] W. W. Qian, C. L. Zhao, S. L. He, X. Y. Dong, S. Q. Zhang, Z. X. Zhang, S. Z. Jin, J. T. Guo, and H. F. Wei, "High-sensitivity temperature sensor based on an alcohol-filled photonic crystal fiber loop mirror," *Optics Letters*, vol. 36, no. 9, pp. 1548–1550, May 2011.

[105] F. Ahmed and M. B. G. Jun, "Microfiber Bragg grating sandwiched between standard optical fibers for enhanced temperature sensing," *IEEE Photonics Technology Letters*, vol. 28, no. 6, pp. 685–688, Mar. 2016.

[106] M. G. Pulido-Navarro, P. J. Escamilla-Ambrosio, S. Marrujo-García, J. A. Álvarez-Chávez, and F. Martínez-Piñón, "Temperature sensing through long period fiber gratings mechanically induced on tapered optical fibers," *Applied Optics*, vol. 56, no. 19, pp. 5526–5531, Jul. 2017.

[107] T. Yamada, Y. Hayamizu, Y. Yamamoto, Y. Yomogida, A. Izadi-Najafabadi, D. N. Futaba, and K. Hata, "A stretchable carbon nanotube strain sensor for human-motion detection," *Nature Nanotechnology*, vol. 6, no. 5, pp. 296–301, Mar. 2011.

[108] L. Cai, L. Song, P. S. Luan, Q. Zhang, N. Zhang, Q. Q. Gao, D. Zhao, X. Zhang, M. Tu, F. Yang, W. B. Zhou, Q. X. Fan, J. Luo, W. Y. Zhou, P. M. Ajayan, and S. S. Xie, "Super-stretchable, transparent carbon nanotube-based capacitive strain sensors for human motion detection," *Scientific Reports*, vol. 3, no. 1, pp. 3048, Oct. 2013.

[109] S. Tadakaluru, W. Thongsuwan, and P. Singjai, "Stretchable and flexible high-strain sensors made using carbon nanotubes and graphite films on natural rubber," *Sensors*, vol. 14, no. 1, pp. 868–876, Jan. 2014.

[110] Q. W. Liu, T. Tokunaga, and Z. Y. He, "Realization of nano static strain sensing with fiber Bragg gratings interrogated by narrow linewidth tunable lasers," *Optics Express*, vol. 19, no. 21, pp. 20214–20223, Oct. 2011.

[111] C. Y. Shen, C. Zhong, J. L. Chu, X. Zou, Y. X. Jin, J. F. Wang, X. Y. Dong, Y. Li, and L. Wang, "Temperature-insensitive strain sensor using a fiber loop mirror based on low-birefringence polarization-maintaining fibers," *Optics Communications*, vol. 287, pp. 31–34, Jan. 2013.

[112] J. Liang and X. H. Sun, "Research and application of twisted optical fiber strain sensor," *Instrument Technique and Sensor*, no. 4, pp. 8–10, Apr. 2015.

[113] F. Xia, Y. Zhao, and M. Q. Chen, "Optimization of Mach-Zehnder interferometer with cascaded up-tapers and application for curvature sensing," *Sensors and Actuators A: Physical*, vol. 263, pp. 140–146, Aug. 2017.

[114] M. Pasquale, "Mechanical sensors and actuators," *Sensors and Actuators A: Physical*, vol. 106, no. 1–3, pp. 142–148, Sep. 2003.

[115] D. Son, S. J. Lim, and C. S. Kim, "Noncontact torque sensor using the difference of maximum induction of amorphous cores," *IEEE Transactions on Magnetics*, vol. 28, no. 5, pp. 2205–2207, Sep. 1992.

[116] R. P. Strittmatter, R. A. Beach, J. Brooke, E. J. Preisler, G. S. Picus, and T. C. Mcgill, "GaN Schottky diodes for piezoelectric strain sensing," *Journal of Applied Physics*, vol. 93, no. 9, pp. 5675–5681, May 2003.

[117] Z. L. Wang, "Self-assembled nanoarchitectures of polar nanobelts/nanowires," *Journal of Materials Chemistry*, vol. 15, no. 10, pp. 1021–1024, Feb. 2005.

[118] M. Benetti, D. Cannata, F. Di Pietrantonio, C. Marchiori, P. Persichetti, and E. Verona, "Pressure sensor based on surface acoustic wave resonators," in *Proceedings of SENSORS, 2008 IEEE*, 2008, pp. 1024–1027.

[119] S. C. Moulzolf, R. Behanan, R. J. Lad, and M. P. da Cunha, "Langasite SAW pressure sensor for harsh environments," in *Proceedings of 2012 IEEE International Ultrasonics Symposium*, 2012, pp. 1224–1227.

[120] J. Schalwig, P. Kreisl, S. Ahlers, and G. Müller, "Response mechanism of SiC-based MOS field-effect gas sensors," *IEEE Sensors Journal*, vol. 2, no. 5, pp. 394–402, Oct. 2002.

[121] O. Casals, B. Barcones, A. Romano-Rodríguez, C. Serre, A. Pérez-Rodríguez, J. R. Morante, P. Godignon, J. Montserrat, and J. Millán, "Characterisation and stabilisation of Pt/TaSi$_x$/SiO$_2$/SiC gas sensor," *Sensors and Actuators B: Chemical*, vol. 109, no. 1, pp. 119–127, Aug. 2005.

[122] R. Bogue, "Nanomaterials for gas sensing: a review of recent research," *Sensor Review*, vol. 34, no. 1, pp. 1–8, Jan. 2014.

[123] F. Mendoza, D. M. Hernández, V. Makarov, E. Febus, B. R. Weiner, and G. Morell, "Room temperature gas sensor based on tin dioxide-carbon nanotubes composite films," *Sensors and Actuators B: Chemical*, vol. 190, pp. 227–233, Jan. 2014.

[124] X. X. Zhang, J. B. Zhang, J. Tang, F. S. Meng, and W. T. Liu, "Ni-doped carbon nanotube sensor for detecting dissolved gases in transformer oil," *Proceedings of the CSEE*, vol. 31, no. 4, pp. 119–124, Feb. 2011.

[125] X. J. Wang, X. X. Zhang, C. X. Sun, and B. Yang, "Surface modification of multi-walled carbon nanotubes by dielectric barrier discharge in atmospheric pressure and the analysis on gas sensitive characteristics," *High Voltage Engineering*, vol. 38, no. 1, pp. 223–228, Jan. 2012.

[126] X. X. Zhang, F. S. Meng, R. H. Li, Y. F. Liao, and B. Yang, "Gas sensitivity studies on hydroxyl modified single-wall carbon nanotube detecting SF$_6$ decomposed components under PD," *High Voltage Engineering*, vol. 39, no. 5, pp. 1069–1074, May 2013.

[127] Y. L. Wu, L. Wang, F. S. Li, H. Y. Zhao, Y. Q. Zhao, and L. Dai, "Preparation and NO$_2$ gas sensing properties of La$_{0.75}$Sr$_{0.25}$Cr$_{0.5}$Mn$_{0.5}$O$_3$," *Journal of the Chinese Rare Earth Society*, vol. 25, no. 5, pp. 562–565, Oct. 2007.

[128] Z. H. Liu, M. L. Wen, Y. Yao, and J. Xiong, "Plastic pethidine hydrochloride membrane sensor and its pharmaceutical applications," *Sensors and Actuators B: Chemical*, vol. 77, no. 3, pp. 219–223, Feb. 2001.

[129] A. Doménech and J. Alarcón, "Determination of hydrogen peroxide using glassy carbon and graphite/polyester composite electrodes modified by vanadium-doped zirconias," *Analytica Chimica Acta*, vol. 425, no. 1, pp. 11–22, Jan. 2002.

[130] N. G. Pavlyukovich, P. A. Murashov, G. N. Dorozhkina, and I. A. Rozanov, "Physicochemical characteristics of the reaction of vapors of organic liquids with divinyl-styrene and isoprene polymer films of piezoelectric chemical sorption sensors," *Journal of Analytical Chemistry*, vol. 55, no. 5, pp. 469–473, May 2000.

[131] P. G. Su, I. C. Chen, and R. J. Wu, "Use of poly(2-acrylamido-2-methylpropane sulfonate) modified with tetraethyl orthosilicate as sensing material for measurement of humidity," *Analytica Chimica Acta*, vol. 449, no. 1–2, pp. 103–109, Dec. 2001.

[132] K. Suri, S. Annapoorni, A. K. Sarkar, and R. P. Tandon, "Gas and humidity sensors based on iron oxide-polypyrrole nanocomposites," *Sensors and Actuators B: Chemical*, vol. 81, no. 2–3, pp. 277–282, Jan. 2002.

[133] M. R. Cavallari, J. E. E. Izquierdo, G. S. Braga, E. A. T. Dirani, M. A. Pereira-da-Silva, E. F. G. Rodríguez, and F. J. Fonseca, "Enhanced sensitivity of gas sensor based on poly(3-hexylthiophene) thin-film transistors for disease diagnosis and environment monitoring," *Sensors*, vol. 15, no. 4, pp. 9592–9609, Apr. 2015.

[134] T. Xie, G. Z. Xie, H. F. Du, Y. Zhou, F. B. Xie, Y. D. Jiang, and H. L. Tai, "The fabrication and optimization of thin-film transistors based on poly(3-hexylthiophene) films for nitrogen dioxide detection," *IEEE Sensors Journal*, vol. 16, no. 7, pp. 1865–1871, Apr. 2016.

[135] A. F. Lv, M. Wang, Y. D. Wang, Z. S. Bo, and L. F. Chi, "Investigation into the sensing process of high-performance H$_2$S sensors based on polymer transistors," *Chemistry-A European Journal*, vol. 22, no. 11, pp. 3654–3659, Mar. 2016.

[136] K. H. Cheon, J. Cho, Y. H. Kim, and D. S. Chung, "Thin film transistor gas sensors incorporating high-mobility diketopyrrolopyrole-based polymeric semiconductor doped with graphene oxide," *ACS Applied Materials & Interfaces*, vol. 7, no. 25, pp. 14004–14010, Jun. 2015.

[137] S. Zampolli, I. Elmi, F. Ahmed, M. Passini, G. C. Cardinali, S. Nicoletti, and L. Dori, "An electronic nose based on solid state sensor arrays for low-cost indoor air quality monitoring applications," *Sensors and Actuators B: Chemical*, vol. 101, no. 1–2, pp. 39–46, Jun. 2004.

[138] W. M. Qu, C. Wenzel, and G, Gerlach, "Fabrication of a 3D differential-capacitive acceleration sensor by UV-LIGA," *Sensors and Actuators A: Physical*, vol. 77, no. 1, pp. 14–20, Sep. 1999.

[139] C. Burbaum, J. Mohr, P. Bley, and W. Ehrfeldabrication of capacitive acceleration sensors by the LIGA technique. *Sensors and Actuators A: Physical*, vol.27, no.1–3, pp. 559–563, 1991.

[140] X. H. Ma and L. Jun, "Design of hybrid integrated capacitive acceleration sensor," in *Proceedings of 2010 International Conference on Electrical and Control Engineering*, 2010, pp. 744–747.

[141] Y. Ohara, M. Miyayama, K. Koumoto, and H. Yanagida, "PZT-polymer piezoelectric composites: a design for an acceleration sensor," *Sensors and Actuators A: Physical*, vol. 36, no. 2, pp. 121–126, Mar. 1993.

[142] J. Terada, "Vibration piezoelectric acceleration sensor," *Journal of the Acoustical Society of America*, vol. 127, no. 3, pp. 1703, Mar. 2010.

[143] R. Amarasinghe, D. V. Dao, V. T. Dau, B. T. Tung, and S. Sugiyama, "Sensitivity enhancement of piezoresistive micro acceleration sensors with Nanometer Stress Concentration Regions on sensing elements," in *Proceedings of 2009 International Solid-State Sensors, Actuators and Microsystems Conference*, 2009, pp. 1333–1336.

[144] S. Vetrivel, R. Mathew, and A. R. Sankar, "Design and optimization of a doubly clamped piezoresistive acceleration sensor with an integrated silicon nanowire piezoresistor," *Microsystem Technologies*, vol. 23, no. 8, pp. 3525–3536, Aug. 2017.

[145] Y. H. Gao, J. Xie, and M. R. Wei, "Structure optimization design of cantilever beam in the piezoresistive acceleration sensor based on artificial neural network," in *Proceedings of 2009 Second International Symposium on Computational Intelligence and Design*, 2009, pp. 254–257.

[146] Y. Tomikawa and S. Okada, "Piezoelectric angular acceleration sensor," in *Proceedings of the IEEE Symposium on Ultrasonics*, 2003, pp. 1346–1349.

[147] A. Gupta, R. Singh, A. Ahmad, and M. Kumar, "Vibration sensors," in *Proceedings of SPIE 5062, Smart Materials, Structures, and Systems*, 2003.

[148] Y. Li, Y. Wang, Q. Cao, J. Cao and D. Qiao, "A Self-Powered Vibration Sensor With Wide Bandwidth," *IEEE Transactions on Industrial Electronics*, vol. 67, no. 1, pp. 560–568, Jan. 2020.

[149] S. Egusa and N. Iwasawa, "Piezoelectric paints: preparation and application as built-in vibration sensors of structural materials," *Journal of Materials Science*, vol. 28, no. 6, pp. 1667–1672, Jan. 1993.

[150] A. M. Vengsarkar, J. A. Greene, B. R. Fogg, and K. A. Murphy, "Spatially weighted, grating-based, two-mode, elliptical-core optical fiber vibration sensors," *Optics Letters*, vol. 16, no. 21, pp. 1707–1709, Nov. 1991.

[151] K. Tanaka, Y. Mochida, M. Sugimoto, K. Moriya, T. Hasegawa, K. Atsuchi, and K. Ohwada, "A micromachined vibrating gyroscope," *Sensors and Actuators A: Physical*, vol. 50, no. 1–2, pp. 111–115, Aug. 1995.

[152] M. N. Armenise, C. Ciminelli, F. Dell'Olio, and V. M. N. Passaro, *Advances in Gyroscope Technologies*, Berlin Heidelberg: Springer, 2011.

[153] K. J. Chen, Z. Y. He, S. X. Wang, J. Hu, L. C. Li, and J. L. He, "Learning-based data analytics: moving towards transparent power grids," *CSEE Journal of Power and Energy Systems*, vol. 4, no. 1, pp. 67–82, Mar. 2018.

[154] A. Hussey, A. Nasipuri, R. Cox, and J. Sorge, "Feasibility of using a wireless mesh sensor network in a coal-fired power plant," in *Proceedings of the IEEE SoutheastCon 2010*, 2010, pp. 384–389.

[155] M. J. Prieto, A. M. Pernía, F. Nuño, J. Díaz, and P. J. Villegas, "Development of a wireless sensor network for individual monitoring of panels in a photovoltaic plant," *Sensors*, vol. 14, no. 2, pp. 2379–2396, Jan. 2014.

[156] A. R. Dyreson, E. R. Morgan, S. H. Monger, and T. L. Acker, "Modeling solar irradiance smoothing for large PV power plants using a 45-sensor network and the Wavelet Variability Model," *Solar Energy*, vol. 110, pp. 482–495, Dec. 2014.

[157] R. J. Bessa, A. Trindade, A. Monteiro, V. Miranda, and C. S. P. Silva, "Solar power forecasting in smart grids using distributed information," in *Proceedings of 2014 Power Systems Computation Conference*, 2014, pp. 1–7.

[158] Y. Amirat, M. E. H. Benbouzid, E. Al-Ahmar, B. Bensaker, and S. Turri, "A brief status on condition monitoring and fault diagnosis in wind energy conversion systems," *Renewable and Sustainable Energy Reviews*, vol. 13, no. 9, pp. 2629–2636, Dec. 2009.

[159] K. J. Chen, J. Hu, Y. Zhang, Z. Q. Yu, and J. L. He, "Fault location in power distribution systems via deep graph convolutional networks," *IEEE Journal on Selected Areas in Communications*, vol. 38, no. 1, pp. 119–131, Jan. 2020.

[160] P. Pinson, "Introducing distributed learning approaches in wind power forecasting," in *Proceedings of 2016 International Conference on Probabilistic Methods Applied to Power Systems*, 2016, pp. 1–6.

[161] L. Duan, J. Hu, G. Zhao, K. J. Chen, J. L. He, and S. X. Wang, "Identification of partial discharge defects based on deep learning method,"

IEEE Transactions on Power Delivery, vol. 34, no. 4, pp. 1557–1568, Aug. 2019.
[162] L. Duan, J. Hu, G. Zhao, K. J. Chen, S. X. Wang, and J. L. He, “Method of inter-turn fault detection for next-generation smart transformers based on deep learning algorithm,” *High Voltage*, vol. 4, no. 4, pp. 282–291, Dec. 2019.
[163] V. C. Gungor, B. Lu, and G. P. Hancke, “Opportunities and challenges of wireless sensor networks in smart grid,” *IEEE Transactions on Industrial Electronics*, vol. 57, no. 10, pp. 3557–3564, Oct. 2010.
[164] A. Nasipuri, R. Cox, J. Conrad, L. Van der Zel, B. Rodriguez, and R. McKosky, “Design considerations for a large-scale wireless sensor network for substation monitoring,” in *Proceedings of the IEEE Local Computer Network Conference*, 2010, pp. 866–873.
[165] R. A. Leon, V. Vittal, and G. Manimaran, “Application of sensor network for secure electric energy infrastructure,” *IEEE Transactions on Power Delivery*, vol. 22, no. 2, pp. 1021–1028, Apr. 2007.
[166] K. J. Chen, C. W. Huang, and J. L. He, “Fault detection, classification and location for transmission lines and distribution systems: a review on the methods,” *High Voltage*, vol. 1, no. 1, pp. 25–33, Apr. 2016.
[167] K. J. Chen, J. Hu, and J. L. He, “A framework for automatically extracting overvoltage features based on sparse autoencoder,” *IEEE Transactions on Smart Grid*, vol. 9, no. 2, pp. 594–604, Mar. 2018.
[168] K. J. Chen, J. Hu, and J. L. He, “Detection and classification of transmission line faults based on unsupervised feature learning and convolutional sparse autoencoder,” *IEEE Transactions on Smart Grid*, vol. 9, no. 3, pp. 1748–1758, May 2018.
[169] Y. Liu, W. X. Yao, D. Zhou, L. Wu, S. T. You, H. S. Liu, L. W. Zhan, J. C. Zhao, H. Y. Lu, W. Gao, and Y. L. Liu, “Recent developments of FNET/GridEye — A situational awareness tool for smart grid,” *CSEE Journal of Power and Energy Systems*, vol. 2, no. 3, pp. 19–27, Sep. 2016.
[170] D. Zhou, J. H. Guo, Y. Zhang, J. D. Chai, H. S. Liu, Y. Liu, C. Huang, X. Gui, and Y. L. Liu, “Distributed data analytics platform for wide-area synchrophasor measurement systems,” *IEEE Transactions on Smart Grid*, vol. 7, no. 5, pp. 2397–2405, Sep. 2016.
[171] C. S. Saunders, G. Y. Liu, Y. Yu, and W. D. Zhu, “Data-driven distributed analytics and control platform for smart grid situational awareness,” *CSEE Journal of Power and Energy Systems*, vol. 2, no. 3, pp. 51–58, Sep. 2016.
[172] K. J. Chen, Q. Wang, Z. Y. He, K. L. Chen, J. Hu, and J. L. He, “Convolutional Sequence to Sequence Non-intrusive Load Monitoring,” *The Journal of Engineering*, vol. 2018, no. 17, pp. 1860–1864, Nov. 2018.
[173] K. J. Chen, K. L. Chen, Q. Wang, Z. Y. He, J. Hu, and J. L. He, “Short-term load forecasting with deep residual networks,” *IEEE Transactions on Smart Grid*, vol. 10, no. 4, pp. 3943–3952, Jul. 2019.
[174] K. J. Chen, Y. Zhang, Q. Wang, J. Hu, H. Fan, and J. L. He, “Scale- and context-aware convolutional non-intrusive load monitoring,” *IEEE Transactions on Power Systems*, vol. 35, no. 3, pp. 2362–2373, May 2020.
[175] J. Hare, X. F. Shi, S. Gupta, and A. Bazzi, “Fault diagnostics in smart micro-grids: a survey,” *Renewable and Sustainable Energy Reviews*, vol. 60, pp. 1114–1124, Jul. 2016.
[176] X. Wang and Q. L. Liang, “Efficient sensor selection schemes for wireless sensor networks in microgrid,” *IEEE Systems Journal*, vol. 12, no. 1, pp. 539–547, Mar. 2018.
[177] S. Y. Wang, J. F. Wan, D. Q. Zhang, D. Li, and C. H. Zhang, “Towards smart factory for industry 4.0: a self-organized multi-agent system with big data based feedback and coordination,” *Computer Networks*, vol. 101, pp. 158–168, Jun. 2016.
[178] M. Brettel, N. Friederichsen, M. Keller, and M. Rosenberg, “How virtualization, decentralization and network building change the manufacturing landscape: an industry 4.0 perspective,” *International Journal of Information and Communication Engineering*, vol. 8, no. 1, pp. 37–44, 2014.
[179] M. F. Li and H. J. Lin, “Design and implementation of smart home control systems based on wireless sensor networks and power line communications,” *IEEE Transactions on Industrial Electronics*, vol. 62, no. 7, pp. 4430–4442, Jul. 2015.
[180] N. K. Suryadevara, S. C. Mukhopadhyay, S. D. T. Kelly, and S. P. S. Gill, “WSN-based smart sensors and actuator for power management in intelligent buildings,” *IEEE/ASME Transactions on Mechatronics*, vol. 20, no. 2, pp. 564–571, Apr. 2015.
[181] F. Viani, F. Robol, A. Polo, P. Rocca, G. Oliveri, and A. Massa “Wireless architectures for heterogeneous sensing in smart home applications: concepts and real implementation,” *Proceedings of the IEEE*, vol. 101, no. 11, pp. 2381–2396, Nov. 2013.
[182] Q. Q. Sun, W. H. Yu, N. Kochurov, Q. Hao, and F. Hu, “A multi-agent-based intelligent sensor and actuator network design for smart house and home automation,” *Journal of Sensor and Actuator Networks*, vol. 2, no. 3, pp. 557–588, Aug. 2013.
[183] K. L. Zhou, S. L. Yang, and C. Shen, “A review of electric load classification in smart grid environment,” *Renewable and Sustainable Energy Reviews*, vol. 24, pp. 103–110, Aug. 2013.
[184] S. Haben, C. Singleton, and P. Grindrod, “Analysis and clustering of residential customers energy behavioral demand using smart meter data,” *IEEE Transactions on Smart Grid*, vol. 7, no. 1, pp. 136–144, Jan. 2016.
[185] R. Pal, C. Chelmis, C. Tadepalli, M. Frincu, S. Aman, and V. Prasanna, “Challenge: on online time series clustering for demand response: optic-a theory to break the ’curse of dimensionality’,” in *Proceedings of the 2015 ACM Sixth International Conference on Future Energy Systems*, 2015, pp. 95–100.
[186] H. H. Goh et al., “Improving the Performance of DC Microgrids by Utilizing Adaptive Takagi-Sugeno Model Predictive Control,” *CSEE Journal of Power and Energy Systems*, vol. 9, no. 4, pp. 1472–1481, Jul. 2023.

Jinliang He received the B.Sc. degree from Wuhan University of Hydraulic and Electrical Engineering, Wuhan, China, the M.Sc. degree from Chongqing University, Chongqing, China, and the Ph.D. degree from Tsinghua University, Beijing, China, all in Electrical Engineering, in 1988, 1991 and 1994, respectively. He became a Lecturer in 1994, and an Associate Professor in 1996, with the Department of Electrical Engineering, Tsinghua University. From 1997 to 1998, he was a Visiting Scientist with Korea Electrotechnology Research Institute, Changwon, South Korea, involved in research on metal oxide varistors and high voltage polymeric metal oxide surge arresters. From 2014 to 2015, he was a Visiting Professor with the Department of Electrical Engineering, Stanford University, Palo Alto, CA, USA. In 2001, he was promoted to a Professor with Tsinghua University. He is currently the Chair with High Voltage and Insulation Technology Research Institute, Tsinghua University. He has authored 8 books and 500 technical papers. His research interests include electromagnetic transient analysis and protection, data deep sensing and big data, and dielectric materials.

Zhifei Han received the B.S. degree in Electrical Engineering from Tsinghua University, Beijing, China in 2018. He is currently working toward the Ph.D. degree in the Department of Electrical Engineering, Tsinghua University. His research interests include piezoelectric effect, electric-field measurement, capacitive-sensing devices and piezoresistive devices.

Jun Hu received B.Sc., M.Sc., and Ph.D. degrees in Electrical Engineering from the Department of Electrical Engineering, Tsinghua University in Beijing, China, in July 1998, July 2000, July 2008. Currently, he is an Associate professor in the same department. His research fields include overvoltage analysis in power system, dielectric materials, surge arrester technology, current sensors and electric field sensors.